Title

The impact of common variants on gene expression in the human brain: from RNA to protein to schizophrenia risk

Authors

Qiuman Liang[1†], Yi Jiang[1,2†], Annie W. Shieh[3], Dan Zhou[4,5], Rui Chen[5], Feiran Wang[1], Meng Xu[1], Mingming Niu[6], Xusheng Wang[7], Dalila Pinto[8,9,10,11], Yue Wang[12], Lijun Cheng[13], Ramu Vadukapuram[14], Chunling Zhang[15], Kay Grennan[16], Gina Giase[17], The PsychENCODE Consortium[‡], Kevin P White[18], Junmin Peng[6], Bingshan Li[5], Chunyu Liu[1,16,19*], Chao Chen[1,20,21,22*], Sidney H. Wang[3*]

Affiliations

1 MOE Key Laboratory of Rare Pediatric Diseases & Hunan Key Laboratory of Medical Genetics, School of Life Sciences, and Department of Psychiatry, The Second Xiangya Hospital, Central South University, Changsha, Hunan 410000, China.

2 Department of Epidemiology and Biostatistics, Ministry of Education Key Laboratory of Environment and Health, School of Public Health, Tongji Medical College, Huazhong University of Science and Technology, Wuhan, Hubei 430000, China.

19 3 Center for Human Genetics, The Brown foundation Institute of Molecular Medicine,
20 The University of Texas Health Science Center at Houston, Houston, TX 77030, USA.

21 4 School of Public Health and the Second Affiliated Hospital, Zhejiang University School
22 of Medicine, Hangzhou, Zhejiang 310058, China.

23 5 Department of Molecular Physiology and Biophysics, Vanderbilt Genetics Institute,
24 Vanderbilt University, Nashville, TN 37232, USA.

25 6 Department of Structural Biology, Department of Developmental Neurobiology, Center
26 for Proteomics and Metabolomics, St. Jude Children's Research Hospital, Memphis, TN 38105,
27 USA.

28 7 Department of Genetics, Genomics, and Informatics, University of Tennessee Health
29 Science Center, Memphis, TN 38163, USA.

30 8 Department of Psychiatry, and Seaver Autism Center for Research and Treatment, Icahn
31 School of Medicine at Mount Sinai, New York, NY 10029, USA.

32 9 Department of Genetics and Genomic Sciences, and Icahn Institute for Data Science and
33 Genomic Technology, Icahn School of Medicine at Mount Sinai, New York, NY 10029, USA.

34 10 The Mindich Child Health and Development Institute, Icahn School of Medicine at
35 Mount Sinai, New York, NY 10029, USA.

36 11 Friedman Brain Institute, Icahn School of Medicine at Mount Sinai, New York, NY
37 10029, USA.

12 Department of Electrical and Computer Engineering, Virginia Polytechnic Institute and State University, Arlington, VA 22203, USA.

13 Institute for Genomics and Systems Biology, University of Chicago, Chicago, IL 60637, USA.

14 Department of Psychiatry, The University of Texas Rio Grande Valley, Harlingen, TX 78550, USA.

15 Department of Neuroscience and Physiology, SUNY Upstate Medical University, Syracuse, NY 13210, USA.

16 Department of Psychiatry, SUNY Upstate Medical University, Syracuse, NY 13210, USA.

17 The Feinberg School of Medicine, Northwestern University, Chicago, IL 60611, USA.

18 Department of Biochemistry, Yong Loo Lin School of Medicine, National University of Singapore, Singapore 117596, Singapore.

19 School of Psychology, Shaanxi Normal University, Xi'an, Shaanxi 710062, China.

20 Furong Laboratory, Changsha, Hunan 410000, China.

21 National Clinical Research Center for Mental Disorders, The Second Xiangya Hospital, Central South University, Changsha, Hunan 410000, China.

22 National Engineering Research Center of Personalized Diagnostic and Therapeutic Technology, Central South University, Changsha, Hunan 410000, China.

† These authors contributed equally to this work.

‡ PsychENCODE Consortium authors and affiliations are listed in the supplementary materials.

* Corresponding author email: **Hsi.Ming.S.Wang@uth.tmc.edu** (S. H. Wang), chenchao@sklmg.edu.cn (C. Chen), LiuCh@upstate.edu (C. Liu)

Abstract

Background

The impact of genetic variants on gene expression has been intensely studied at the transcription level, yielding in valuable insights into the association between genes and the risk of complex disorders, such as schizophrenia (SCZ). However, the downstream impact of these variants and the molecular mechanisms connecting transcription variation to disease risk are not well understood.

Results

We quantitated ribosome occupancy in prefrontal cortex samples of the BrainGVEX cohort. Together with transcriptomics and proteomics data from the same cohort, we performed cis-Quantitative Trait Locus (QTL) mapping and identified 3,253 expression QTLs (eQTLs), 1,344 ribosome occupancy QTLs (rQTLs), and 657 protein QTLs (pQTLs) out of 7,458 genes quantitated in all three omics types from 185 samples. Of the eQTLs identified, only 34% have their effects propagated to the protein level. Further analysis on the effect size of prefrontal cortex eQTLs identified from an independent dataset showed clear post-transcriptional attenuation of eQTL effects. To investigate the biological relevance of the attenuated eQTLs, we identified 70 expression-specific QTLs (esQTLs), 51 ribosome-occupancy-specific QTLs (rsQTLs), and 107

protein-specific QTLs (psQTLs). Five of these omics-specific QTLs showed strong colocalization with SCZ GWAS signals, three of them are esQTLs. The limited number of GWAS colocalization discoveries from omics-specific QTLs and the apparent prevalence of eQTL attenuation prompted us to take a complementary approach to investigate the functional relevance of attenuated eQTLs. Using S-PrediXcan we identified 74 SCZ risk genes, 34% of which were novel, and 67% of these risk genes were replicated in a MR-Egger test. Notably, 52 out of 74 risk genes were identified using eQTL data and 70% of these SCZ-risk-gene-driving eQTLs show little to no evidence of driving corresponding variations at the protein level.

Conclusion

The effect of eQTLs on gene expression in the prefrontal cortex is commonly attenuated post-transcriptionally. Many of the attenuated eQTLs still correlate with SCZ GWAS signal. Further investigation is needed to elucidate a mechanistic link between attenuated eQTLs and SCZ disease risk.

Introduction

Complex diseases such as neuropsychiatric disorders are multi-factorial with genetic components (*1*, *2*). Large scale Genome-Wide Association Studies (GWAS) have uncovered thousands of disease associated loci, signaling a promising era ahead for causal variant identification (*3*). However, efforts in fine mapping these disease risk loci often narrowed down the underlying causal signals to non-coding regions of the genome (*4–6*). Regulatory variants in such non-coding regions are therefore the prime candidates for driving the genetic risk of disease etiology. Consequently, integrating gene expression information to pinpoint causal variants or to identify risk genes has become a staple of genetic studies of complex diseases (*7*), with multiple consortia

103 efforts facilitating large scale gene expression profiling and regulatory element mapping (*8–10*).
104 Many powerful methods, such as *coloc*, PrediXcan, SMR/HEIDI, to name a few, have also been
105 developed to leverage gene expression information for fine mapping GWAS signals or for
106 identifying underlying risk genes (*11–13*).

107 Schizophrenia (SCZ) is a psychiatric disorder affecting ~1% of the world-wide population (*14*).
108 The heritability of SCZ has been estimated at between 60% to 80% indicating a strong genetic
109 component (*15*, *16*). Accordingly, recent SCZ GWAS study reported by Trubetskoy et al.
110 identified 287 significant risk loci and prioritized 120 risk genes using functional genomic data
111 (*17*). The use of RNA-Seq data from the brain was instrumental for risk gene prioritization by
112 Trubetskoy et al.; however, information from downstream gene regulation processes, such as
113 translation rate and protein abundance, was either not utilized or unavailable.

114 Measuring transcriptional changes as a proxy for gene activity has a long history in molecular
115 biology (*18*). In the context of human genetics, buffering of downstream effects of genetic
116 variants impacting gene expression (i.e. an eQTL) has been shown to be prevalent (*19*). In
117 addition, QTLs specific to protein level have also been reported (*19-21*). Together, these
118 observations indicated the importance and potential benefits of including downstream omics
119 types, such as proteomics data, as information sources for fine mapping disease regulatory
120 variants. Indeed, recent studies using multi-omics approaches have demonstrated increased power
121 for risk gene identification among other benefits (*22*, *23*). Of note, our recent work on genetic
122 variants associated with protein level in prefrontal cortex of the human brain indicated the extent
123 of contribution from non-synonymous coding variants to changes at the protein level, and the
124 utility of these protein QTL variants in prioritizing GWAS risk genes for psychiatric disorders
125 (*21*).

126 Another potential benefit of taking a multi-omics approach for identifying disease risk genes rests
127 in the potential to dissect the fine details of regulatory mechanisms driving the disease-genotype
128 association. Having relevant datasets to illuminate the origin and propagation of genetic impact
129 could potentially arrive at a conclusion of the driver regulatory process for a risk gene. Ribo-seq
130 is a technology that can be used to collect relevant data to fill in the gap between transcript and
131 protein expression. By adapting RNA-Seq to a ribosome footprinting method, ribo-seq provides
132 transcriptome-wide quantification of ribosome occupancy (*24*, *25*), which can serve as a proxy for
133 the amount of active translation synthesizing proteins from each mRNA transcript. When
134 analyzed in conjunction with RNA-Seq and quantitative proteomics data, ribo-seq enables
135 identification of translational and post-translational regulatory events (*19, 26*), both major steps
136 defining the human genetics aspect of the Central Dogma of molecular biology.

137 As a part of the consortium efforts to improve our understanding of the genetic basis of
138 neuropsychiatric disorders (*27*), we generated multiple data modalities that included SNP
139 genotyping, RNA-Seq, ribo-seq, and proteomics of postmortem cortical tissue samples of the
140 BrainGVEX cohort, which altogether covered all major observables of the Central Dogma. In
141 conjunction with the quantitative proteomics and transcriptome profiling results that we
142 previously published (*21*, *28*), here we integrated ribo-seq data as our operational definition for
143 protein synthesis, based on the ribosome occupancy level across the transcriptome, to advance our
144 multi-omics investigation. Our results reveal regulatory properties of common variants in the
145 human brain and their utility in identifying the regulatory processes driving disease risk for
146 schizophrenia. It offers an opportunity to dissect and appreciate the regulatory information flow in
147 the biological processes associated with the Central Dogma from a population perspective.
148 Additional "rules" including an effect attenuation process is recognized.

149 **Results**

150 *Measuring transcriptome-wide ribosome occupancy level in prefrontal cortex of adult human*
151 *brain to quantify the level of protein translation*

152 To investigate regulatory impact of genetic variants on protein translation in the prefrontal cortex
153 of the human brain, we performed ribosome profiling on 211 prefrontal cortex samples from the
154 BrainGVEX collection. In total we collected ~62 billion ribosome profiling reads. Consistent with
155 the expected ribosome footprint size, we found the average insert size of our ribo-seq libraries to
156 range between 27.4 and 29.5 nucleotides. Similar to prior published studies (*29*), we found on
157 average 74 % of unwanted reads from ribosomal RNA, tRNA, and snoRNA, which contributed
158 no information to the translation of protein coding genes. After removing these unwanted reads,
159 we obtained an average of 30.3 million uniquely mapped informative reads per sample (inter-
160 quartile range: 20.5 ~ 37.6 million reads). When focusing our analysis on the informative reads,
161 we found our ribo-seq data to have ~3 times higher proportion of exon reads than that of the total
162 RNA-Seq data collected from the same individuals using an rRNA-depletion method (*28*). When
163 visualized in aggregate across annotated coding genes, we found our ribo-seq data to show strong
164 sub-codon periodicity at the expected positions (Fig. S1). High proportion of exon reads and
165 strong sub-codon periodicity indicates the enrichment of footprints from ribosomes actively
166 engaged in translating mature mRNA and reflects the quality of the dataset.

167 *Multi-omics cis-QTL mapping identified candidate regulatory variants and revealed translational*
168 *and post-translational attenuation of eQTL effects*

169 To identify variants associated with inter-individual expression differences, we perform cis-QTL
170 mapping for each omics type independently. Using the full dataset (i.e. 416 RNA-Seq samples,
171 195 ribo-seq samples, and 268 proteomics samples, and the corresponding genotype data), we
172 identified 12,411 eQTLs (out of 16,540 genes we deem sufficiently quantitated), 2,849 rQTLs

173 (out of 14,572 genes), and 1,036 pQTLs (out of 8,013 genes) at FDR < 0.1. The majority of the
174 eQTLs identified here were replicated in the prefrontal cortex RNA-Seq data from the GTEx
175 consortium (Table S1). Intriguingly, we found drastic differences between omics types in the
176 numbers of QTLs mapped, suggesting that some of the eQTL effects do not propagate all the way
177 to the protein level. However, the differences in the number of genes tested between omics types
178 and the differences in sample size make the comparison challenging to interpret. To better
179 compare the effects of genetic regulation between multiple data modalities, we identified 185
180 samples with 7,458 genes that were sufficiently quantitated across all three omics types. Using
181 this unified dataset, we found 3,253 eQTLs, 1,344 rQTLs, and 657 pQTLs at FDR <0.1 (Fig. 1A,
182 Fig. S2, Table S2, S3, S4). Similar to the results derived from the full dataset, using the unified
183 dataset we found fewer significant QTLs as we moved downstream the Central Dogma of
184 molecular biology.

185 A challenge in comparing between the numbers of QTLs identified from each omics type rests in
186 the fact that not all true effects were identified. Tests replicating QTLs identified from one omics
187 type in the other omics types can better capture the proportion of genetic effects shared between
188 QTL types. We performed replication tests using $\pi 1$ estimates from the qvalue method (*30*).
189 Overall, we found high proportion of QTLs replicated in other omics types (Fig. 1B). However,
190 when considering the replication rates with the direction of genetic information flow, we found
191 asymmetric replication rates, with the downstream omics types to replicate less than the upstream
192 omics types. More specifically, we found 84.7% of the rQTLs were replicated at the transcript
193 level, but only 60.2% of the eQTLs were replicated at the ribosome occupancy level. Moreover,
194 while 75.9% of the pQTLs were replicated at the transcript level, only 34.0% of the eQTLs were
195 replicated at the protein level (Fig. 1B). The lower percentages of eQTLs and rQTLs replicated at
196 the protein level indicate potential effect attenuation (i.e. either the inter-individual variation in
197 gene expression becoming smaller and therefore harder to detect or a lack of such effect in the

198 downstream omics types). Interestingly, in addition to the effect attenuation at the protein level,
199 which was previously reported for lymphoblastoid cell lines (LCLs) (*19*), here, using brain
200 samples, we found further asymmetry between eQTL and rQTL replication, indicating effect
201 attenuation at the level of translation. A similar asymmetry in proportion replicated between
202 upstream and downstream omics types was observed when using a direction-aware cutoff-based
203 approach across a wide range of significance cutoffs used to define replication rates (Fig. S3).

204 While our replication tests revealed a trend of effect attenuation for eQTL variants in the
205 downstream phenotypes (Fig. 1B), these same observations could alternatively be explained by
206 differences in statistical power between technologies. An independent piece of evidence that is
207 not sensitive to measurement precision is needed to reach a solid conclusion. Using eQTLs
208 independently identified from prefrontal cortex samples by the CommonMind Consortium (CMC)
209 (*31*), we avoid the ascertainment bias for large effect size eQTLs identified from our dataset and
210 can therefore directly compare the effects size of eQTL variants between the three omics types
211 using our dataset. A similar approach was successfully implemented to address this power issue in
212 previous work in LCLs (*19*). Using 5,915 CMC eQTLs that were also quantitated in our dataset,
213 we found the eQTL effects on the transcript expression level to be significantly larger than their
214 effects on ribosome occupancy level (per allele log2 fold differences: mRNA 0.2433 [95% CI=
215 0.2381~0.2486] vs. ribosome occupancy 0.1836 [95% CI= 0.1794~0.1878]), which were in turn
216 significantly larger than their effects on protein level (per allele log2 fold differences: 0.1486
217 [95% CI= 0.1451~0.1522]) (Fig. 1C, t-test $P < 2.2e^{-16}$ for all pairwise comparisons). By focusing
218 on the effect sizes of independently identified eQTLs, our results strongly support the presence of
219 downstream mechanisms attenuating eQTL effects both at the ribosome occupancy level
220 (translationally) and at the protein level (post-translationally). Moreover, for the CMC eQTLs, we
221 found translational regulation to account for more effect size reduction than post-translational
222 regulation (Fig. 1C).

223 *Identifying omics specific QTLs and their signal colocalization with schizophrenia GWAS*

224 The prevalent effect size reduction of eQTLs raised the question of the relevance of these genetic
225 regulation at the organismal level. Because most cellular tasks are executed by proteins, the
226 genetic regulatory effects not reaching the protein level are, presumably, less likely to have an
227 impact on organismal traits. To answer this question, we set out to investigate the relevance of
228 different QTL types in SCZ. More specifically, we aim to identify expression specific QTLs (i.e.
229 genetic variants that impact transcript level of the linked genes but not the downstream ribosome
230 occupancy level nor protein level) that colocalize with SCZ GWAS.

231 Consistent with prior reports (*32*), using our full dataset we found significant proportion of SCZ
232 heritability to be mediated by gene expression. By performing mediated expression score
233 regression (MESC) (*32*) on summary statistics from the Trubetskoy et al. SCZ GWAS (*17*), we
234 found our eQTLs to mediate 7.09%, rQTLs to mediate 4.06%, and pQTLs to mediate 2.17% of
235 SCZ heritability (Table S5). After establishing the relevance for each of the three QTL types in
236 SCZ, we next sought to identify omics-specific QTLs, in order to further evaluate their relevance
237 in driving SCZ risk. Because regulation of a gene is often modulated by multiple genetic variants,
238 to evaluate the consequence of overall *cis*-QTL impact on gene expression, we use PrediXcan to
239 estimate aggregate genetic regulatory effects for each gene. To distinguish between genes that
240 have QTL effects shared across multiple omics types and genes that have omics-specific QTL
241 effects, for each omics type we built PrediXcan models with or without regressing out the other
242 omics types and computed the correlation between the imputed expression from the two models.
243 We termed this correlation R_c. To identify R_c^2 values that reflect significant sharing between
244 omics types, we permuted sample labels to emulate conditions of no real correlation between the
245 three omics types, in order to generate empirical null distributions. Using both a false discovery
246 rate (FDR), which is calculated based on the empirical null, and an effect size cutoff based on R_c^2,

247 we defined a set of shared QTL genes and three sets of omics-specific QTL genes. At 10% FDR,
248 we defined shared QTL genes by further requiring the R_c^2 to be smaller than 0.5. Using these
249 criteria, from the 1,354 genes that passed the minimum PrediXcan criteria for being included in
250 this analysis (see details in methods), we identified 295 shared QTL genes that have QTL effects
251 shared between at least two omics types. For genes that failed to reject null at the 10% FDR cutoff
252 (i.e. potentially omics-specific) we further set a conservative $R_c^2 > 0.9$ cutoff to define omics-
253 specific QTLs for those QTLs that did not change after regressing out effects from other omics
254 types. Using these criteria, we found 70 esQTL (mRNA-specific QTL) genes, 51 rsQTL
255 (ribosome occupancy-specific QTL) genes, and 107 psQTL (protein-specific QTL) genes (Fig.
256 S4, Table S6).

257 To investigate the relevance of omics-specific QTL genes in SCZ, we performed summary
258 statistics-based signal colocalization between QTL signals and SCZ GWAS signals. Using *coloc*
259 with default prior (*11*), at a posterior probability cutoff of 70% for the signal colocalization
260 hypothesis, we found esQTLs of 3 genes, *CCDC117, GATAD2A,* and *JAKMIP2* to colocalize
261 with SCZ GWAS signals at loci *22q12.1*, *19p13.11,* and *5q32*, respectively (Fig. 2A, Fig. 2B). In
262 addition, we found rsQTLs of *UGGT2* to colocalize with SCZ GWAS signals at locus *13q32.1*
263 (Fig. 2C, Fig. 2D) and psQTLs of *P2RX7* to colocalize with SCZ GWAS signals at locus
264 *12q24.31*. On the other hand, for shared QTL genes, we found the eQTLs of 6 genes and the
265 rQTLs of 1 gene to colocalize with SCZ GWAS signals. In summary, we identified strong signal
266 colocalization with SCZ GWAS from both shared QTLs and omics-specific QTLs, at comparable
267 proportions (i.e. 7 from 295 of shared vs. 5 from 228 of omics-specific), indicating the relevance
268 of omics-specific QTLs in explaining SCZ GWAS signals.

269 *Functional genomics identification of Schizophrenia risk genes*

270 To further investigate the relevance of attenuated eQTLs in SCZ risk, we next took a
271 complementary approach by first identifying risk genes from each omics type separately and then
272 investigating the relevant regulatory processes driving SCZ risk. Following the observed
273 percentages of SCZ heritability mediated by gene regulation found in our full dataset, here using
274 the same GWAS we focused our effort to identify risk genes for SCZ based on our unified multi-
275 omics dataset using S-PrediXcan (*33*). At 5% family-wise error rate, we found 52, 29, and 16
276 SCZ risk genes, respectively from RNA-Seq, ribo-seq, and proteomics data (Fig. 3A, Fig. S5;
277 note that the color and shape coding of this figure will become relevant in the next results
278 section). Among them only four genes, *NEK4*, *KHK*, *CNNM2* and *DARS2* were consistently
279 identified as SCZ risk genes from all three omics types (Fig. 3B). The majority (74.3%) of the
280 risk genes were identified only from one of the three omics types. This limited sharing in risk
281 gene identification between omics types is in clear contrast to the amount of signal sharing found
282 between QTL types (Fig. 1B).

283 Among the 74 risk genes we identified using S-PrediXcan (i.e. the union of the risk genes
284 identified from each of the three omics types), 44 have previously been reported in GWAS studies
285 as either the mapped genes or as one of the nearby genes under the GWAS peak (Table S7) (*17*,
286 *34–36*). Of these previously reported genes, 27 matched the mapped genes while the remaining 17
287 nominated an alternative candidate gene for each GWAS locus (Note that for some of these 17
288 loci, the original GWAS signals were mapped to an intergenic region). Comparing our results to
289 other published SCZ risk gene identification studies, we found 15 matched to the risk genes
290 identified by Giambartolomei et al., which used RNA-Seq and DNA methylation data from
291 prefrontal cortex of the human brain (*22*) and 12 matched to the 120 prioritized SCZ risk genes
292 from Trubetskoy et al., which used colocalization with eQTL and Hi-C data (*17*). On the other
293 hand, for 25 of our 74 risk genes (33.8%), we found no match to the known risk gene list (Table
294 S8), which we compiled based on previous GWAS and functional genomics risk gene

295 identification studies (*17*, *22*, *34–36*). These "no match" novel risk genes have relatively weak
296 SCZ GWAS signals and are therefore challenging to identify without the additional information
297 provided by our multi-omics QTL dataset. For example, we found strong colocalization between a
298 modest SCZ GWAS signal at *2p23.3* and all three types of molecular QTLs of the gene *KHK*
299 (Fig. 3D). Intriguingly, the *KHK* pQTL is in opposite direction of the *KHK* eQTL and rQTL (Fig.
300 3C), suggesting a linked post-translational process regulating the protein level in addition to the
301 transcriptional regulation. *KHK*, Ketohexokinase, plays a pivotal role in fructose metabolism and
302 has been hypothesized to contribute to neuronal glycolysis and the loss of neuronal functions (*37*).
303 In addition to *KHK*, other novel SCZ risk genes have also been reported to participate in neuronal/
304 cognitive functions: Overexpression of *BTN3A2,* Butyrophilin Subfamily 3 member A2, was
305 found to inhibit excitatory synaptic activity in CA1 pyramidal neurons (*38*). *NSF*, N-
306 Ethylmaleimide Sensitive Factor, which encodes a vesicle fusing ATPase, was reported as a
307 causal factor in intelligence traits (*39*).

308 *Analyses of multi-omics dataset reveal regulatory mechanisms of schizophrenia risk genes*

309 While PrediXcan is a powerful tool for GWAS risk gene identification, it does not control for
310 potential horizontal pleiotropy (*40*). To this end, we performed two-sample Mendelian
311 Randomization (MR) with Egger regression to replicate the risk genes we identified using S-
312 PrediXcan. Egger regression includes an intercept term, which can be used to evaluate the level of
313 horizontal pleiotropy (*41*). For each risk gene we first used LD-clumping (*42*) to identify top
314 SNPs from independent signals as strong genetic instruments (*43*). We then tested for the causal
315 relationship between gene regulation (i.e. QTL signal) and SCZ (i.e. GWAS). We used an
316 operational definition of a causal effect based on the MR test results (see Methods). At 10% FDR,
317 of the 97 gene-by-omics combinations (i.e. a total of 74 risk genes including some discovered
318 from more than one omics type), 67.0% (65/97) passed the MR test. Of those 33.0% that failed

319 the MR test, 93.8% (30 out of 32) failed because of horizontal pleiotropy identified by the Egger
320 intercept test (Table S9). A total of 52 genes were replicated in at least one of the three omics
321 types. Similar, but stronger, causal effects were observed when using SuSiE (the Sum of Single
322 Effects) (*44*) as an alternative approach to define instrument SNPs (Fig. S6). However, when
323 using SuSiE for selecting instrument variables, only 41 genes were tested because some of the
324 risk genes had no fine mapped QTL SNPs according to SuSiE.

325 A key strength of using a multi-omics QTL approach to identify GWAS risk genes rests in the
326 possibility of further narrowing down the potential regulatory mechanisms. To this end, we
327 further examined the likely causal mechanisms for the 52 replicated SCZ risk genes using one-
328 sample Mendelian Randomization to infer causality between QTL types. We focused our analysis
329 on independently testing for causal effects between neighboring QTL types following the
330 direction of information flow of the Central Dogma (i.e. mRNA -> ribosome occupancy, and
331 ribosome occupancy -> protein). Here we used fine-mapped QTL SNPs identified from the
332 exposure omics types (i.e. the upstream omics types) as instrument variables for one-sample MR
333 analysis. Among the 52 MR-Egger replicated SCZ risk genes, we found 17 genes with significant
334 causal effects both from eQTL to rQTL (i.e. the upstream pathway) and from rQTL to pQTL (i.e.
335 the downstream pathway) (both-passed risk genes; Fig. 3A dark red solid circle datapoints).
336 Significant causal effects detected from both pathways suggest transcriptionally regulated protein
337 level differences as the potential mechanisms driving these risk genes in SCZ etiology (see an
338 example in Fig. 4A, Fig. 4B). On the other hand, 27 and 8 replicated risk genes have either
339 significant causal effects only in one of the two pathways (single-passed risk genes; Fig. 3A blue
340 triangle datapoints) or have no significant causal effects (none-passed risk genes; Fig. 3A orange
341 rectangle datapoints), respectively.

342 Of note, for the 27 single-passed risk genes, we found significant causal effects only in the
343 upstream pathway (mRNA -> ribosome occupancy). This asymmetry is reminiscent of the eQTL
344 effect attenuation described in the prior sections. A failed test could indicate either a true lack of
345 effect or a lack of statistical power. To take a closer look, we directly assessed the effect size, the
346 noise level, and instrument strength of the one-sample MR test results. When comparing to the 17
347 both-passed risk genes, we found significantly smaller effect sizes both for failed tests of the 27
348 single-passed risk genes (only the downstream MR test results included, average 0.367 vs 0.055,
349 t-test $P < 4.9e^{-5}$, Fig. S7A) and the 8 none-passed risk genes (both upstream and downstream MR
350 test results included, average 0.405 vs 0.033, t-test $P < 4e^{-12}$, Fig. S8A). Note that in both cases
351 the inter-quartile range of the estimated causal effects for the failed tests covered zero (Fig. S7A,
352 Fig. S8A). On the other hand, for these same comparison groups, we found no significant
353 difference in instrument strength (Fig. S7C, S8C, if anything slightly stronger instrument was
354 observed in failed tests) and found only slightly higher noise level in the failed MR tests (Fig.
355 S7B and S8B; t-test P = 0.026 and P= 0.013 respectively). The estimated small causal effects
356 from the failed tests indicate that either we are observing weak effects that are obscured by the
357 slightly elevated noise level (false negatives) or a lack of true causal effects, or a mixture of the
358 two. In other words, some of these risk genes are likely to be driven by specific QTL types. Case
359 in point, we found *SF3B1* to have similar patterns in p value distributions between eQTLs and
360 SCZ GWAS but no clear QTL signals in either ribo-seq or proteomics data (Fig. 4C, Fig. 4D).

361 **Discussion**

362 Using a panel of postmortem prefrontal cortex samples, we found clear evidence of post-
363 transcriptional attenuation of eQTL effects in the human brain. Many of the differences found
364 between individual brain transcriptomes were not present between individual brain proteomes.
365 This observation echoes earlier work in HapMap lymphoblastoid cell lines (*19*) and extends the

366 prior conclusion from *in vitro* cell lines to complex human tissues. Importantly, distinct from the
367 earlier work in lymphoblastoid cell lines, which found translation to mostly track with
368 transcription, we found clear attenuation of eQTL effect in ribo-seq data indicating that
369 translational regulatory processes are involved in eQTL effect attenuation in the human brain.
370 Prevalent translational attenuation of variant impact on transcriptional gene expression level has
371 previously been reported in budding yeast (*45*, *46*). However, results from follow up studies (*47*)
372 appear to present an inconsistent picture. Here, using replication tests for individual eQTLs and
373 testing for aggregate effect size of eQTLs independently identified from CMC, we provided
374 strong evidences supporting prevalent translational attenuation of eQTL effects in the human
375 brain. Although operating at the molecular level, our study remained observational. Omics-
376 specific features could potentially confound the results. Future work replicating this observation
377 and elucidating molecular mechanisms of translational attenuation of eQTL effects are needed to
378 provide a clear understanding of the phenomenon.

379 Following this observation, our current work focuses on the important question of whether the
380 attenuated eQTLs are functionally (biologically) relevant. We attempted to address this question
381 by exploring the relevance of attenuated eQTLs in SCZ, a neuropsychiatric disorder that is highly
382 heritable. We took two approaches to identify risk genes that have either omics-specific QTL
383 signals or attenuated eQTLs. In the first approach, we used PrediXcan to aggregate variant impact
384 at the gene level, in order to identify omics-specific risk genes. Our method is distinct from
385 published work on omics-specific QTLs that took a SNP-based approach (*19*). Using a gene-
386 based approach, we aimed to increase the interpretability of the results and decrease the challenge
387 of the needle in the haystack problem. Indeed, our approach reduced our search space to 1,354
388 genes, and among these genes we identified 228 omics-specific QTL genes. By limiting our
389 search to the most confident set of omics-specific QTL genes, we identified three clear examples
390 of esQTLs that show strong colocalization with SCZ GWAS signals. At the same time, the

391 limited number of discoveries put certain constraints on our ability to investigate the properties of
392 esQTLs in the context of SCZ disease risk. It is expected that a better powered study with a larger
393 sample size would reveal more esQTLs and enable a deeper mechanistic investigation.

394 In the second approach, we expanded our search by first identified risk genes from all quantitated
395 genes using a TWAS approach, S-PrediXcan method. We then replicated the TWAS risk genes
396 using two-sample Mendelian Randomization with Egger intercept tests. While the majority of the
397 TWAS risk genes were replicated in two-sample Mendelian Randomization tests, of the minority
398 that failed the MR tests most failed because of the Egger intercept test. Our results, therefore,
399 clearly confirmed the need of controlling for potential horizontal pleiotropy in TWAS studies
400 (*41*). About 34% of the risk genes that we identified here have not been previously reported as
401 SCZ risk genes. The use of our functional genomics dataset is key to the discovery of these novel
402 SCZ risk genes because of their relatively weak GWAS signals (see Fig. 3D for an example). To
403 identify causal regulatory mechanisms for each replicated risk gene, we further tested causality
404 between QTL types using one-sample MR. We found 17 risk genes that are likely contributing to
405 SCZ risk through transcriptionally regulated protein level. On the other hand, we also identify 8
406 genes that show no significant results from MR tests (candidate omics-specific risk genes) and 27
407 genes that have significant MR test results only from transcription to translation (candidate post-
408 translationally-attenuated risk genes).

409 In essence, attempts to identify esQTLs (or any omics-specific QTLs) are dealing with the
410 challenge of separating true negatives from false negatives. While we applied very conservative
411 criteria to identify esQTLs and performed subsequent evaluations, such caveat is important to
412 keep in mind when interpreting our results. Similarly, the interpretation of the failed MR tests is
413 challenging. Our subsequent analyses looking at comparing instrument strength, noise level, and
414 effect size between passed and failed MR tests, indicated comparable instrument strength, slightly

415 elevated noise level in the failed tests, and clearly smaller effect size in the failed tests. In other
416 words, it remains possible that some of the failed tests could be reflecting a small effect size
417 obscured by the elevated noise level. In addition to the issues with false negative results, some of
418 the discoveries could be false positives to begin with. Although we have good confidence with
419 our FDR and FWER estimates, given that our test statistics for QTL mapping and risk gene
420 identification are well calibrated (Fig. S2, S5), pleiotropy could introduce positive results from a
421 different underlying cause (i.e. true effects on SCZ risk but false positive risk genes).

422 Power issues, however, do not explain the whole story. As was consistently observed throughout
423 our study, when viewed in aggregate, we see clear effect size differences between omics types,
424 both for QTLs and for causal effects from MR tests. These effect size estimates are not influenced
425 by significance cutoffs and are not biased by power differences. Such general trends are also
426 unlikely to simply be a result of spurious associations or made up entirely of false positives. Our
427 results therefore bring forth an interesting mechanistic question: how do attenuated eQTL variants
428 impact SCZ without changing protein levels? One interesting possibility is that the biologically
429 relevant traits here are translation efficiency (i.e. protein synthesis rates) and protein turnover
430 rates. An association between genotype and translation efficiency could manifest in the form of an
431 attenuated eQTL, where the differences in translation rate appears to offset the differences
432 introduced at the transcript level, which in turn resulted in a lack of association between eQTL
433 SNP genotype and ribosome occupancy level. In other words, the colocalization between an
434 attenuated eQTL and GWAS signal could be reflecting a colocalization of GWAS signal with a
435 translation efficiency QTL. Similarly a protein turnover QTL could also manifest in the form of a
436 rQTL attenuated at the protein level. This hypothesis would predict additional linked regulatory
437 variants (i.e. linked to the attenuated eQTLs) that impact translation efficiency or protein turnover
438 rates. We hope by presenting the current results, our findings can inspire future studies on this
439 topic to better understand the regulatory processes from DNA to diseases.

440 **Materials and Methods**

441 **Data sources**

442 The SNP genotypes (*21*), RNA-Seq (*28*), and quantitative mass spectrometry (*21*) data generated
443 for prefrontal cortex tissue samples of the BrainGVEX cohort were downloaded from the
444 PsychENCODE Synapse portal (https://www.synapse.org/#!Synapse:syn5613798) (See Table
445 S10 for a summary on the number of samples in each dataset and their respective overlap with the
446 samples in the genotype data). The BrainGVEX cohort includes 420 Caucasians, 2 Hispanics, 1
447 African American, 3 Asian Americans, and 14 unknown-origin individuals. We also used PGC3
448 SCZ GWAS summary statistics data obtained from the Psychiatric Genomics Consortium (*17*).

449 **Ribosome profiling**

450 Ribosome Profiling experiments were performed using Illumina's TrueSeq Ribo Profile
451 (Mammalian) Kit. TrueSeq Ribo Profile (Mammalian) Kit was developed for cell lines. We
452 adapted the protocol to frozen tissue samples with MP Biomedicals™ FastPrep-24™ Classic
453 Bead Beating Grinder and Lysis System. Specifically, 60-80 mg of frozen brain tissue was
454 homogenized in Lysing Matrix D tubes containing 800 µl polysome lysis buffer. The Lysing
455 tubes were placed on the FastPrep-24™ homogenizer set at 4.0 m/s with 20 s increments until no
456 visible chunks of tissue remained. Tissue lysate was incubated on ice for 10 min followed by
457 centrifugation at 20,000g at 4 °C for 10 minutes to pellet cell debris. Clarified lysate was
458 subsequently used for ribo-seq library preparation following TrueSeq Ribo Profile (Mammalian)
459 Kit instructions. Indexed libraries were pooled and then sequenced on an Illumina HiSeq 4000.
460 Note that the experimental protocol for TrueSeq Ribo Profile (Mammalian) Kit that we followed
461 is a modified version of the previous ribo-seq protocol published by Ingolia and colleagues (*25*),
462 and it has the following key modifications: Monosome isolation was performed using Sephacryl

463 S400 spin columns (GE; 27–5140-01) on a tabletop centrifuge instead of ultra-high speed
464 centrifugation in sucrose cushion. Ribosomal RNA depletion was carried out by using Ribo-Zero
465 Magnetic Kits and this step is moved up to right after the monosomal RNA isolation step and
466 before the Ribosome Protected Fragment gel isolation step.

467 **Data processing, gene expression quantification, and normalization**

468 For RNA-Seq data, we obtained the FASTQ raw data from the PsychENCODE BrainGVEX
469 project (https://www.synapse.org/#!Synapse:syn5613798). Then we used cutadapt (v1.12) to trim
470 adapter for raw reads with code "cutadapt –minimum-length=5 –quality-base=33 -q 30 -a
471 AGATCGGAAGAGCACACGTCTGAACTCCAGTCA -A
472 AGATCGGAAGAGCGTCGTGTAGGGAAAGAGTGT". Then we mapped trimmed reads onto
473 GENCODE Release 19 (GRCh37.p13) genome with same version's GTF by STAR (v2.4.2a).
474 Then we used RSEM software (v1.2.29) to quantify the read counts for each gene (*48*). The cpm
475 function in the R package "limma" was used to calculate the log-transformed counts per million
476 (CPM). We filtered out the genes with CPM < 1 in more than 75% samples and the samples with
477 network connectivity (*49*) z score < -5 (Fig. S9), which resulted in a total of 17,207 genes from
478 426 samples in the quantification table. We then used normalize.quantiles function in the R
479 package "preprocessCore" (*50*) to normalize expression level for each sample. We used DRAMS
480 software to detect and correct mixed-up samples (*41*), which resulted in final 423 samples.

481 For ribo-seq data, we used cutadapt (v1.12) to trim adapter for raw reads with code "cutadapt -a
482 AGATCGGAAGAGCACACGTCT –quality-base=33 –minimum-length=25 –discard-
483 untrimmed". The trimmed reads were then mapped against a FASTA file of rRNA, tRNA, and
484 snoRNA sequence downloaded from NCBI using bowtie2 (*52*) to filter out uninformative reads.
485 The filtered reads were mapped to GENCODE Release 19 (GRCh37.p13) genome with

corresponding transcript model GTF file using STAR (v2.4.2a). The uniquely mapped reads, as defined by the "NH:i:1" flag of the alignment files, were kept for subsequent analysis. We used the featureCounts function in the R package "subreads" (*53*) to calculate gene level read counts for ribosome occupancy. The cpm function in the R package "limma" was used to calculate log-transformed CPM value. We filtered out genes with CPM < 1 in more than 75% samples and the samples with network connectivity (*49*) z score < -3.5 (Fig. S10), which resulted in a total of 15,171 genes quantitated from 209 samples in the quantification table. We then used the normalize.quantiles function in the R package "preprocessCore" (*50*) to normalize ribosome occupancy level for each sample. We used DRAMS software to detect and correct mixed-up samples (*51*), which resulted in 199 samples.

For quantitative mass spectrometry data, we obtained protein quantification table from the PsychENCODE BrainGVEX Synapse portal (https://www.synapse.org/#!Synapse:syn5613798). This table includes abundance quantification for 11,572 proteins from 268 samples. The data processing steps for producing the mass spectrometry quantification table is detailed in Luo et al. (*21*). We further log-transformed protein abundance for each sample. We filtered out genes with log-transformed protein abundance < 1 in more than 75% samples and the samples with network connectivity (*49*) z score < -6, and found no gene and sample were filtered out. We then used the normalize.quantiles function in the R package "preprocessCore" (*50*) to normalize protein level for each sample. We used DRAMS software to detect and correct mixed-up samples (*51*), which found no mixed-up samples. We matched the protein ID to gene ID according to the UCSC database of hg19 version, which resulted in 8,330 genes.

QTL mapping

Estimating and adjusting for unwanted factors

509 We used the R package "PEER" (*54*) to estimate hidden factors for RNA-Seq, ribo-seq, and
510 proteomics data separately. The principle of selecting unwanted hidden factors was to maximize
511 the variance explained with the least number of factors. We identified 30, 29, and 19 hidden
512 factors to remove from RNA-Seq, ribo-seq, and mass spectrometry data, respectively (Fig. S11).
513 For each gene from each omics type, we adjusted the expression level by fitting the selected
514 hidden factors as predictors in a linear model and taking the residuals as the adjusted expression
515 level. The adjusted expression levels were then further centered by mean and scaled by standard
516 deviation.

517 *Genotype association tests*

518 We identified *cis*-region expression QTLs (*cis*-eQTLs), ribosome occupancy QTLs (*cis*-rQTLs),
519 and protein QTLs (*cis*-pQTLs) separately using QTLTools (1.3.1) (*55*). Because each gene can
520 encode several protein isoforms, we selected the protein isoform with the highest median
521 abundance as the representative protein. For each gene, we defined *cis*-region as the region
522 ranging from 1Mb upstream of the 5' end of the gene to 1Mb downstream of the 3' end of the
523 gene (i.e. the length of the gene body plus 2 Mb in size). We tested all common SNPs (MAF >
524 0.05) within the *cis*-region using 10,000 permutations to create empirical null distributions and
525 used the beta-approximation approach implemented in QTLTools to estimate the empirical p
526 values. For each gene, we selected the SNP with the most significant empirical p value from the
527 genotype-expression level association tests to represent the QTL signal. To calculate a genome-
528 wide FDR, we used the qvalue function of the R package "qvalue" for multiple testing correction
529 and set a qvalue < 0.1 (i.e. 10% FDR) cutoff to identify significant QTLs.

530 **Estimating mediated SCZ heritability of each omics**

531 We used MESC to estimate the proportion of SCZ heritability mediated by different omics (*32*).
532 In the first step, we calculated the overall expression score using the unwanted-factor-adjusted-
533 expression data (see QTL mapping section) as the individual-level gene expression data with the
534 corresponding BrainGVEX genotype data and the 1000 genome phase 3 genotype data as the
535 ancestry matched genotype data for GWAS. In the second step, we used the overall expression
536 score calculated in the previous step and PGC3 SCZ GWAS summary statistics to estimate SCZ
537 heritability mediated by each omics.

538 **Identifying shared and omics-specific QTL genes**

539 *Building PrediXcan gene expression prediction models*

540 We used the PrediXcan software (*13*) to separately build gene expression prediction models for
541 RNA-Seq, ribo-seq, and proteomics. For each gene, an Elastic Net algorithm was used for feature
542 selection from SNPs located within the *cis*-region defined for each gene (i.e. gene body +/- 1Mb
543 flanking regions) based on results from a ten-fold cross-validation. After that, weights were
544 produced for every selected SNP of each gene, which were used in the prediction models. For
545 each gene, we calculated the Pearson correlation between predicted and observed gene expression
546 (Cross-validation R, R_{cv}), which was considered as a metric for prediction accuracy. Only the
547 genes with $R_{cv} > 0.1$ and $P < 0.05$ were retained. We produced prediction models for the unified
548 set of 7,458 genes and 185 samples shared across omics.

549 *Building conditionally independent prediction models*

550 To identify shared and omics-specific QTL genes among different omics, we built conditionally
551 independent prediction models for each omics. For each gene, we regressed from the data the
552 genetic regulation signals of all other omics types (i.e. the imputed quantification level of all other

omics types). The models were built based on the regressed expression (i.e. the residual from the regression). Note that because in many cases multiple protein isoform quantifications match to one gene, when building model for gene-based quantification omics types, such as mRNA and ribosome occupancy, we aggregate data across all protein isoforms for each gene. In contrast, when building model for protein data, quantifications between isoforms were kept separate.

More specifically, assuming a total of p omics types, we took the following steps to identify shared-QTL genes and to define omics-specific QTL genes:

Step 1: For each gene and each omics type, we built original prediction models using equation 1

$$E_k = \sum_{i=0}^{n} w_i S_i + \varepsilon, \quad (1)$$

where E_k denotes the observed expression of omics type k; w_i denotes the weight of the i-th SNP S_i; n denotes the number of SNPs selected by the elastic net.

We can calculate the imputed expression with genotype data: $\widehat{E_k} = \sum_{i=0}^{n} w_i S_i$.

Step 2: For each gene in omics type k, we regressed out the imputed expression on the same gene of all the other omics types from the observed expression using equation 2 and kept the residual

$$E_k = \beta_1 \widehat{E_1} + \beta_2 \widehat{E_2} + \cdots + \beta_{l-1} \widehat{E_{l-1}} + e_k, \quad (2)$$

where β_l denotes slope of the l-th other omics types, $\widehat{E_l}$ denotes the imputed expression of the l-th other omics types, and e_k denotes the residual for omics type k. Then, we calculated the expression value conditioning on the genetic regulation of all the other omics types: $R_k = \overline{E_k} + e_k$. Where $\overline{E_k}$ is the sum of mean expression across genes.

572 Step 3: After that, we built the conditional prediction models and estimated the SNP-weights
573 parameters) using equation 3.

574 $$R_k = \sum_{i=0}^{n} m_i S_i + \varepsilon, \quad (3)$$

575 where m_i is the weight of i-th SNP S_i for the conditional prediction model.

576 Step 4: We calculated the square of correlation of imputed gene expression between the original
577 model and conditional model and named it as observed R_c^2.

578 Step 5: To determine whether a gene share genetic regulation signals with other omics types, we
579 used permutation to create a null distribution of R_c^2. We permuted the sample label for imputed
580 expression of the other omics types, and repeated step 2to build the conditional prediction model
581 using permuted data, which we named conditional permutation model. We then calculated
582 permutation R_c^2 of imputed gene expression between the original model and conditional
583 permutation model.

584 Step 6: We performed 50 permutations and calculated empirical p values of the observed R_c^2
585 based on its rank among the permutation R_c^2 (i.e. ordered from the smallest to the greatest).

586 Step 7: We used Benjamini-Hochberg control procedure to adjust the empirical p values to
587 calculate FDR for shared-QTL genes.

588 Step 8: We defined omics-specific QTL genes as genes with FDR > 0.1 and R_c^2 >0.9, and the
589 omics-shared QTL genes as genes with FDR <0.1 and R_c^2 <0.5.

590 **Colocalization**

591 We used *coloc* (*11*) to detect signal colocalization between SCZ GWAS and each QTL type at the
592 cis-region of each QTL gene. For each QTL gene, for all common SNPs (MAF > 0.05) within the
593 cis-region, we use QTL effects and GWAS summary statistics as input for coloc analysis. For
594 QTL effects, we calculated slope and square of slope' standard error from a linear model fit using
595 SNP genotype as the predictor of gene quantifications. We then used the coloc.abf function in the
596 R package "*coloc*" (*11*) to calculate the posterior possibility of each hypothesis using the default
597 prior. We use posterior probability of 70% for the colocalization hypothesis (i.e. PPH4) as the
598 cutoff for reporting our colocalization findings.

599 **TWAS identification of SCZ risk genes**

600 Gene-level association tests were performed for SCZ using S-PrediXcan (*33*) based on the
601 prediction models built using our omics data, which is described in the "building prediction
602 models" section, and the SCZ GWAS summary statistics data from PGC3 (*17*). The association
603 tests were done separately for each omics. For protein data, we performed omnibus test to
604 incorporate p values of all protein isoforms together to calculate a single p value for the
605 corresponding gene. The family wise error rates for SCZ risk genes were calculated using
606 Bonferroni correction of nominal p values.

607 **Two-sample Mendelian randomization (MR)**

608 To identify causal relationships between each omics type and SCZ we used MR analysis. Here we
609 used fine mapped QTL SNPs as instruments, gene expression quantification at each omics type as
610 exposure, and SCZ GWAS signal as outcome.

611 More specifically, we took the following steps to test for causal relationship between gene
612 regulation at each omics level and SCZ:

613 Step 1: Here we used two methods of selecting instrument SNPs. For each gene of each QTL
614 type, we performed LD clumping by PLINK with "–clump-kb 1000 –clump-r2 0.5" parameters to
615 select instrument SNPs with p value < 0.05. Another method is fine-mapping by susie_rss()
616 function with default parameters in R package "SuSiE" (*44*).

617 Step 2: For each gene, we used harmonise_data() function in R package "TwoSampleMR" (*56*) to
618 harmonize QTLs of each omics type and SCZ GWAS SNPs to be in the same direction (i.e. effect
619 relative to the same allele).

620 Step 3: We then performed two-sample MR for each gene in each omics type separately. Two-
621 sample MR analysis was done using mr() function, which includes IVW and Egger methods, in
622 the R package "TwoSampleMR" (*56*).

623 Step 4: We used the intercept test (i.e. the Egger method) to test for horizontal pleiotropy, and
624 used predictor coefficient and its corresponding p value from IVW to determine the effect size
625 and significance of causal effects for each omics type on SCZ.

626 Step 5: We used Benjamini-Hochberg to adjust for multiple testing.

627 Step 6: We define a gene by omics type combination as causal for SCZ if the causal effect test
628 passed the FDR < 0.1 cutoff and the Egger intercept test passed the intercept p value > 0.05
629 cutoff.

630 **One-sample Mendelian randomization**

631 For one-sample MR we used two-stage least squares (2SLS) approach to find causal relationships
632 between omics types. We performed the following analysis in two iterations, both following the
633 direction of genetic information flow. In the first iteration, we tested causal relationships between

transcript level and ribosome occupancy level (i.e. mRNA -> ribosome occupancy). In the second iteration, we tested causal relationships between ribosome occupancy level and protein level (i.e. ribosome occupancy -> protein).

Step 1: We used the same two methods for instrument SNP selection as described in the previous section. Here we tested two pathways (mRNA -> ribosome occupancy and ribosome occupancy -> protein). For mRNA -> ribosome occupancy, we used the SNPs of eQTL with p value < 0.05 and LD clumping by PLINK with "–clump-kb 1000 –clump-r2 0.5" parameters. For ribosome occupancy -> protein, we used the SNPs of rQTL with p value < 0.05 and LD clumping by PLINK with "–clump-kb 1000 –clump-r2 0.5".

Step 2: We then combined genotype and quantification data of the relevant omics types into a dataframe: dat_{mr} for mRNA -> ribosome occupancy pathway, dat_{rp} for ribosome occupancy -> protein pathway.

Step 3: For each gene, we then set formula in R package "ivreg": ivreg("ribosome occupancy ~ mRNA | SNP_1+SNP_2+SNP_3+…+SNP_n", data = dat_{mr}) and ivreg("protein ~ ribosome occupancy | SNP_1+SNP_2+SNP_3+…+SNP_m", data = dat_{rp}).

Step 4: We used the summary() function to get slope, p value of slope, intercept, p value of intercept, F-statistic and p value of F-statistic of each ivreg object. P value of Intercept was used to test horizontal pleiotropy, F-statistic was used to check instrument strength.

Step 5: We used Benjamini-Hochberg control procedure to adjust for multiple testing.

Step 6: We defined a causal relationship for each gene by pathway combination as the causal effect test passed the FDR < 0.1 cutoff and the Egger intercept test passed the intercept p value > 0.05 cutoff.

656 **References**

657 1. A. Fialkowski, T. M. Beasley, H. K. Tiwari, "[11 – Multifactorial Inheritance and Complex Diseases]" in
658 *Emery and Rimoin's Principles and Practice of Medical Genetics and Genomics (Seventh Edition)*, R. E.
659 Pyeritz, B. R. Korf, W. W. Grody, Eds. (Academic Press, 2019), pp. 323–358.

660 2. A. S. Brown, The environment and susceptibility to schizophrenia. *Prog. Neurobiol*. 93, 23–58 (2011).

661 3. N. Solovieff, C. Cotsapas, P. H. Lee, S. M. Purcell, J. W. Smoller, Pleiotropy in complex traits: challenges and
662 strategies. *Nat. Rev. Genet.* 14, 483–495 (2013).

663 4. K. Watanabe, E. Taskesen, A. van Bochoven, D. Posthuma, Functional mapping and annotation of genetic
664 associations with FUMA. *Nat. Commun.* 8, 1826 (2017).

665 5. M. G. Heckman, C. Labbé, A. L. Kolicheski, A. I. Soto-Beasley, R. L. Walton, R. R. Valentino, E. R. Brennan,
666 P. W. Johnson, S. Baheti, V. Sarangi, Y. Ren, R. J. Uitti, Z. K. Wszolek, O. A. Ross, Fine-mapping of the non-
667 coding variation driving the Caucasian LRRK2 GWAS signal in Parkinson's disease. *Parkinsonism Relat.*
668 *Disord*. 83, 22–30 (2021).

669 6. D. J. Schaid, W. Chen, N. B. Larson, From genome-wide associations to candidate causal variants by statistical
670 fine-mapping. *Nat. Rev. Genet.* 19, 491–504 (2018).

671 7. A. Gusev, A. Ko, H. Shi, G. Bhatia, W. Chung, B. W. J. H. Penninx, R. Jansen, E. J. C. de Geus, D. I.
672 Boomsma, F. A. Wright, P. F. Sullivan, E. Nikkola, M. Alvarez, M. Civelek, A. J. Lusis, T. Lehtimäki, E.
673 Raitoharju, M. Kähönen, I. Seppälä, O. T. Raitakari, J. Kuusisto, M. Laakso, A. L. Price, P. Pajukanta, B.
674 Pasaniuc, Integrative approaches for large-scale transcriptome-wide association studies. *Nat. Genet.* 48, 245–
675 252 (2016).

676 8. M. Fromer, P. Roussos, S. K. Sieberts, J. S. Johnson, D. H. Kavanagh, T. M. Perumal, D. M. Ruderfer, E. C.
677 Oh, A. Topol, H. R. Shah, L. L. Klei, R. Kramer, D. Pinto, Z. H. Gümüş, A. E. Cicek, K. K. Dang, A. Browne,

678 C. Lu, L. Xie, B. Readhead, E. A. Stahl, J. Xiao, M. Parvizi, T. Hamamsy, J. F. Fullard, Y.-C. Wang, M. C.
679 Mahajan, J. M. J. Derry, J. T. Dudley, S. E. Hemby, B. A. Logsdon, K. Talbot, T. Raj, D. A. Bennett, P. L. De
680 Jager, J. Zhu, B. Zhang, P. F. Sullivan, A. Chess, S. M. Purcell, L. A. Shinobu, L. M. Mangravite, H.
681 Toyoshiba, R. E. Gur, C.-G. Hahn, D. A. Lewis, V. Haroutunian, M. A. Peters, B. K. Lipska, J. D. Buxbaum,
682 E. E. Schadt, K. Hirai, K. Roeder, K. J. Brennand, N. Katsanis, E. Domenici, B. Devlin, P. Sklar, Gene
683 expression elucidates functional impact of polygenic risk for schizophrenia. *Nat. Neurosci*. 19, 1442–1453
684 (2016).

685 9. ENCODE Project Consortium, J. E. Moore, M. J. Purcaro, H. E. Pratt, C. B. Epstein, N. Shoresh, J. Adrian, T.
686 Kawli, C. A. Davis, A. Dobin, R. Kaul, J. Halow, E. L. Van Nostrand, P. Freese, D. U. Gorkin, Y. Shen, Y. He,
687 M. Mackiewicz, F. Pauli-Behn, B. A. Williams, A. Mortazavi, C. A. Keller, X.-O. Zhang, S. I. Elhajjajy, J.
688 Huey, D. E. Dickel, V. Snetkova, X. Wei, X. Wang, J. C. Rivera-Mulia, J. Rozowsky, J. Zhang, S. B. Chhetri,
689 J. Zhang, A. Victorsen, K. P. White, A. Visel, G. W. Yeo, C. B. Burge, E. Lécuyer, D. M. Gilbert, J. Dekker, J.
690 Rinn, E. M. Mendenhall, J. R. Ecker, M. Kellis, R. J. Klein, W. S. Noble, A. Kundaje, R. Guigó, P. J. Farnham,
691 J. M. Cherry, R. M. Myers, B. Ren, B. R. Graveley, M. B. Gerstein, L. A. Pennacchio, M. P. Snyder, B. E.
692 Bernstein, B. Wold, R. C. Hardison, T. R. Gingeras, J. A. Stamatoyannopoulos, Z. Weng, Expanded
693 encyclopaedias of DNA elements in the human and mouse genomes. *Nature*. 583, 699–710 (2020).

694 10. GTEx Consortium, The GTEx Consortium atlas of genetic regulatory effects across human tissues. *Science*.
695 369, 1318–1330 (2020).

696 11. C. Giambartolomei, D. Vukcevic, E. E. Schadt, L. Franke, A. D. Hingorani, C. Wallace, V. Plagnol, Bayesian
697 test for 31etwork31renia31 between pairs of genetic association studies using summary statistics. *PloS Genet*.
698 10, e1004383 (2014).

699 12. E. R. Gamazon, H. E. Wheeler, K. P. Shah, S. V. Mozaffari, K. Aquino-Michaels, R. J. Carroll, A. E. Eyler, J.
700 C. Denny, D. L. Nicolae, N. J. Cox, H. K. Im, A gene-based association method for mapping traits using
701 reference transcriptome data. *Nat. Genet*. 47, 1091–1098 (2015).

13. Z. Zhu, F. Zhang, H. Hu, A. Bakshi, M. R. Robinson, J. E. Powell, G. W. Montgomery, M. E. Goddard, N. R. Wray, P. M. Visscher, J. Yang, Integration of summary data from GWAS and eQTL studies predicts complex trait gene targets. *Nat. Genet*. 48, 481–487 (2016).

14. R. S. Kahn, I. E. Sommer, R. M. Murray, A. Meyer-Lindenberg, D. R. Weinberger, T. D. Cannon, M. O 'Donovan, C. U. Correll, J. M. Kane, J. van Os, T. R. Insel, Schizophrenia. *Nat. Rev. Dis. Primers*. 1, 15067 (2015).

15. P. Lichtenstein, B. H. Yip, C. Björk, Y. Pawitan, T. D. Cannon, P. F. Sullivan, C. M. Hultman, Common genetic determinants of schizophrenia and bipolar disorder in Swedish families: a population-based study. *Lancet*. 373, 234–239 (2009).

16. P. F. Sullivan, K. S. Kendler, M. C. Neale, Schizophrenia as a complex trait: evidence from a meta-analysis of twin studies. *Arch Gen Psychiatry*. 60, 1187–1192 (2003).

17. V. Trubetskoy, A. F. Pardiñas, T. Qi, G. Panagiotaropoulou, S. Awasthi, T. B. Bigdeli, J. Bryois, C.-Y. Chen, C. A. Dennison, L. S. Hall, M. Lam, K. Watanabe, O. Frei, T. Ge, J. C. Harwood, F. Koopmans, S. Magnusson, A. L. Richards, J. Sidorenko, Y. Wu, J. Zeng, J. Grove, M. Kim, Z. Li, G. Voloudakis, W. Zhang, M. Adams, I. Agartz, E. G. Atkinson, E. Agerbo, M. Al Eissa, M. Albus, M. Alexander, B. Z. Alizadeh, K. Alptekin, T. D. Als, F. Amin, V. Arolt, M. Arrojo, L. Athanasiu, M. H. Azevedo, S. A. Bacanu, N. J. Bass, M. Begemann, R. A. Belliveau, J. Bene, B. Benyamin, S. E. Bergen, G. Blasi, J. Bobes, S. Bonassi, A. Braun, R. A. Bressan, E. J. Bromet, R. Bruggeman, P. F. Buckley, R. L. Buckner, J. Bybjerg-Grauholm, W. Cahn, M. J. Cairns, M. E. Calkins, V. J. Carr, D. Castle, S. V. Catts, K. D. Chambert, R. C. K. Chan, B. Chaumette, W. Cheng, E. F. C. Cheung, S. A. Chong, D. Cohen, A. Consoli, Q. Cordeiro, J. Costas, C. Curtis, M. Davidson, K. L. Davis, L. de Haan, F. Degenhardt, L. E. DeLisi, D. Demontis, F. Dickerson, D. Dikeos, T. Dinan, S. Djurovic, J. Duan, G. Ducci, F. Dudbridge, J. G. Eriksson, L. Fañanás, S. V. Faraone, A. Fiorentino, A. Forstner, J. Frank, N. B. Freimer, M. Fromer, A. Frustaci, A. Gadelha, G. Genovese, E. S. Gershon, M. Giannitelli, I. Giegling, P. Giusti-Rodríguez, S. Godard, J. I. Goldstein, J. González Peñas, A. González-Pinto, S. Gopal, J. Gratten, M. F. Green, T. A. Greenwood, O. Guillin, S. Gülöksüz, R. E. Gur, R. C. Gur, B. Gutiérrez, E. Hahn, H. Hakonarson, V. Haroutunian, A. M. Hartmann, C. Harvey, C. Hayward, F. A. Henskens, S.

Herms, P. Hoffmann, D. P. Howrigan, M. Ikeda, C. Iyegbe, I. Joa, A. Julià, A. K. Kähler, T. Kam-Thong, Y. Kamatani, S. Karachanak-Yankova, O. Kebir, M. C. Keller, B. J. Kelly, A. Khrunin, S.-W. Kim, J. Klovins, N. Kondratiev, B. Konte, J. Kraft, M. Kubo, V. Kučinskas, Z. A. Kučinskiene, A. Kusumawardhani, H. Kuzelova-Ptackova, S. Landi, L. C. Lazzeroni, P. H. Lee, S. E. Legge, D. S. Lehrer, R. Lencer, B. Lerer, M. Li, J. Lieberman, G. A. Light, S. Limborska, C.-M. Liu, J. Lönnqvist, C. M. Loughland, J. Lubinski, J. J. Luykx, A. Lynham, M. Macek, A. Mackinnon, P. K. E. Magnusson, B. S. Maher, W. Maier, D. Malaspina, J. Mallet, S. R. Marder, S. marsal, A. R. Martin, L. Martorell, M. Mattheisen, R. W. McCarley, C. McDonald, J. J. McGrath, H. Medeiros, S. Meier, B. Melegh, I. Melle, R. I. Mesholam-Gately, A. Metspalu, P. T. Michie, L. Milani, V. Milanova, M. Mitjans, E. Molden, E. Molina, M. D. Molto, V. Mondelli, C. Moreno, C. P. Morley, G. Muntané, K. C. Murphy, I. Myin-Germeys, I. Nenadić, G. Nestadt, L. Nikitina-Zake, C. Noto, K. H. Nuechterlein, N. L. O'Brien, F. A. O'Neill, S.-Y. Oh, A. Olincy, V. K. Ota, C. Pantelis, G. N. Papadimitriou, M. Parellada, T. Paunio, R. Pellegrino, S. Periyasamy, D. O. Perkins, B. Pfuhlmann, O. Pietiläinen, J. Pimm, D. Porteous, J. Powell, D. Quattrone, D. Quested, A. D. Radant, A. Rampino, M. H. Rapaport, A. Rautanen, A. Reichenberg, C. Roe, J. L. Roffman, J. Roth, M. Rothermundt, B. P. F. Rutten, S. Saker-Delye, V. Salomaa, J. Sanjuan, M. L. Santoro, A. Savitz, U. Schall, R. J. Scott, L. J. Seidman, S. I. Sharp, J. Shi, L. J. Siever, E. Sigurdsson, K. Sim, N. Skarabis, P. Slominsky, H.-C. So, J. L. Sobell, E. Söderman, H. J. Stain, N. E. Steen, A. A. Steixner-Kumar, E. Stögmann, W. S. Stone, R. E. Straub, F. Streit, E. Strengman, T. S. Stroup, M. Subramaniam, C. A. Sugar, J. Suvisaari, D. M. Svrakic, N. R. Swerdlow, J. P. Szatkiewicz, T. M. T. Ta, A. Takahashi, C. Terao, F. Thibaut, D. Toncheva, P. A. Tooney, S. Torretta, S. Tosato, G. B. Tura, B. I. Turetsky, A. Üçok, A. Vaaler, T. van Amelsvoort, R. van Winkel, J. Veijola, J. Waddington, H. Walter, A. Waterreus, B. T. Webb, M. Weiser, N. M. Williams, S. H. Witt, B. K. Wormley, J. Q. Wu, Z. Xu, R. Yolken, C. C. Zai, W. Zhou, F. Zhu, F. Zimprich, E. C. Atbaşoğlu, M. Ayub, C. Benner, A. Bertolino, D. W. Black, N. J. Bray, G. Breen, N. G. Buccola, W. F. Byerley, W. J. Chen, C. R. Cloninger, B. Crespo-Facorro, G. Donohoe, R. Freedman, C. Galletly, M. J. Gandal, M. Gennarelli, D. M. Hougaard, H.-G. Hwu, A. V. Jablensky, S. A. McCarroll, J. L. Moran, O. Mors, P. B. Mortensen, B. Müller-Myhsok, A. L. Neil, M. Nordentoft, M. T. Pato, T. L. Petryshen, M. Pirinen, A. E. Pulver, T. G. Schulze, J. M. Silverman, J. W. Smoller, E. A. Stahl, D. W. Tsuang, E. Vilella, S.-H. Wang, S. Xu, R. Adolfsson, C. Arango, B. T. Baune, S. I. Belangero, A. D. Børglum, D. Braff, E. Bramon, J. D. Buxbaum, D. Campion, J. A. Cervilla, S. Cichon, D. A. Collier, A. Corvin, D. Curtis, M. D. Forti, E. Domenici, H. Ehrenreich, V. Escott-Price, T. Esko, A. H. Fanous, A. Gareeva, M. Gawlik, P. V. Gejman, M. Gill, S. J. Glatt, V. Golimbet, K. S. Hong, C. M. Hultman, S. E. Hyman, N. Iwata,

758 E. G. Jönsson, R. S. Kahn, J. L. Kennedy, E. Khusnutdinova, G. Kirov, J. A. Knowles, M.-O. Krebs, C.
759 Laurent-Levinson, J. Lee, T. Lencz, D. F. Levinson, Q. S. Li, J. Liu, A. K. Malhotra, D. Malhotra, A.
760 McIntosh, A. McQuillin, P. R. Menezes, V. A. Morgan, D. W. Morris, B. J. Mowry, R. M. Murray, V.
761 Nimgaonkar, M. M. Nöthen, R. A. Ophoff, S. A. Paciga, A. Palotie, C. N. Pato, S. Qin, M. Rietschel, B. P.
762 Riley, M. Rivera, D. Rujescu, M. C. Saka, A. R. Sanders, S. G. Schwab, A. Serretti, P. C. Sham, Y. Shi, D. St
763 Clair, H. Stefánsson, K. Stefansson, M. T. Tsuang, J. van Os, M. P. Vawter, D. R. Weinberger, T. Werge, D.
764 B. Wildenauer, X. Yu, W. Yue, P. A. Holmans, A. J. Pocklington, P. Roussos, E. Vassos, M. Verhage, P. M.
765 Visscher, J. Yang, D. Posthuma, O. A. Andreassen, K. S. Kendler, M. J. Owen, N. R. Wray, M. J. Daly, H.
766 Huang, B. M. Neale, P. F. Sullivan, S. Ripke, J. T. R. Walters, M. C. O'Donovan, Mapping genomic loci
767 implicates genes and synaptic biology in schizophrenia. *Nature*. 604, 502–508 (2022).

768 18. J. B. W. Wolf, Principles of transcriptome analysis and gene expression quantification: an RNA-seq tutorial.
769 *Mol Ecol Resour*. 13, 559–572 (2013).

770 19. A. Battle, Z. Khan, S. H. Wang, A. Mitrano, M. J. Ford, J. K. Pritchard, Y. Gilad, Impact of regulatory
771 variation from RNA to protein. *Science*. 347, 664–667 (2015).

772 20. E. Ferkingstad, P. Sulem, B. A. Atlason, G. Sveinbjornsson, M. I. Magnusson, E. L. Styrmisdottir, K.
773 Gunnarsdottir, A. Helgason, A. Oddsson, B. V. Halldorsson, B. O. Jensson, F. Zink, G. H. Halldorsson, G.
774 Masson, G. A. Arnadottir, H. Katrinardottir, K. Juliusson, M. K. Magnusson, O. T. Magnusson, R.
775 Fridriksdottir, S. Saevarsdottir, S. A. Gudjonsson, S. N. Stacey, S. Rognvaldsson, T. Eiriksdottir, T. A.
776 Olafsdottir, V. Steinthorsdottir, V. Tragante, M. O. Ulfarsson, H. Stefansson, I. Jonsdottir, H. Holm, T. Rafnar,
777 P. Melsted, J. Saemundsdottir, G. L. Norddahl, S. H. Lund, D. F. Gudbjartsson, U. Thorsteinsdottir, K.
778 Stefansson, Large-scale integration of the plasma proteome with genetics and disease. *Nat. Genet*. 53, 1712–
779 1721 (2021).

780 21. J. Luo, M. Niu, L. Li, D. Kong, Y. Jiang, A. Shieh, L. Cheng, G. Giase, K. Grennan, K. White, C. Chen, S.
781 Wang, D. Pinto, Y. Wang, C. Liu, J. Peng, X. Wang, https://doi.org/10.21203/rs.3.rs-1633422/v1 (2022).

782 22. C. Giambartolomei, J. Zhenli Liu, W. Zhang, M. Hauberg, H. Shi, J. Boocock, J. Pickrell, A. E. Jaffe,
783 CommonMind Consortium, B. Pasaniuc, P. Roussos, A Bayesian framework for multiple trait colocalization
784 from summary association statistics. *Bioinformatics*. 34, 2538–2545 (2018).

785 23. C. N. Foley, J. R. Staley, P. G. Breen, B. B. Sun, P. D. W. Kirk, S. Burgess, J. M. M. Howson, A fast and
786 efficient colocalization algorithm for identifying shared genetic risk factors across multiple traits. *Nat.*
787 *Commun*. 12, 764 (2021).

788 24. N. T. Ingolia, S. Ghaemmaghami, J. R. S. Newman, J. S. Weissman, Genome-wide analysis in vivo of
789 translation with nucleotide resolution using ribosome profiling. *Science*. 324, 218–223 (2009).

790 25. N. T. Ingolia, G. A. Brar, S. Rouskin, A. M. McGeachy, J. S. Weissman, The ribosome profiling strategy for
791 monitoring translation in vivo by deep sequencing of ribosome-protected mRNA fragments. *Nat. Protoc*. 7,
792 1534–1550 (2012).

793 26. Cenik C, Cenik ES, Byeon GW, Grubert F, Candille SI, Spacek D, Alsallakh B, Tilgner H, Araya CL, Tang H,
794 Ricci E, Snyder MP. Integrative analysis of RNA, translation, and protein levels reveals distinct regulatory
795 variation across humans. *Genome Res.* 25, 1610-1621 (2015).

796 27. S. Akbarian, C. Liu, J. A. Knowles, F. M. Vaccarino, P. J. Farnham, G. E. Crawford, A. E. Jaffe, D. Pinto, S.
797 Dracheva, D. H. Geschwind, J. Mill, A. C. Nairn, A. Abyzov, S. Pochareddy, S. Prabhakar, S. Weissman, P. F.
798 Sullivan, M. W. State, Z. Weng, M. A. Peters, K. P. White, M. B. Gerstein, A. Amiri, C. Armoskus, A. E.
799 Ashley-Koch, T. Bae, A. Beckel-Mitchener, B. P. Berman, G. A. Coetzee, G. Coppola, N. Francoeur, M.
800 Fromer, R. Gao, K. Grennan, J. Herstein, D. H. Kavanagh, N. A. Ivanov, Y. Jiang, R. R. Kitchen, A.
801 Kozlenkov, M. Kundakovic, M. Li, Z. Li, S. Liu, L. M. Mangravite, E. Mattei, E. Markenscoff-Papadimitriou,
802 F. C. P. Navarro, N. North, L. Omberg, D. Panchision, N. Parikshak, J. Poschmann, A. J. Price, M. Purcaro, T.
803 E. Reddy, P. Roussos, S. Schreiner, S. Scuderi, R. Sebra, M. Shibata, A. W. Shieh, M. Skarica, W. Sun, V.
804 Swarup, A. Thomas, J. Tsuji, H. van Bakel, D. Wang, Y. Wang, K. Wang, D. M. Werling, A. J. Willsey, H.
805 Witt, H. Won, C. C. Y. Wong, G. A. Wray, E. Y. Wu, X. Xu, L. Yao, G. Senthil, T. Lehner, P. Sklar, N.
806 Sestan, The PsychENCODE project. *Nat. Neurosci*. 18, 1707–1712 (2015).

807 28. M. J. Gandal, P. Zhang, E. Hadjimichael, R. L. Walker, C. Chen, S. Liu, H. Won, H. van Bakel, M. Varghese,
808 Y. Wang, A. W. Shieh, J. Haney, S. Parhami, J. Belmont, M. Kim, P. Moran Losada, Z. Khan, J. Mleczko, Y.
809 Xia, R. Dai, D. Wang, Y. T. Yang, M. Xu, K. Fish, P. R. Hof, J. Warrell, D. Fitzgerald, K. White, A. E. Jaffe,
810 PsychENCODE Consortium, M. A. Peters, M. Gerstein, C. Liu, L. M. Iakoucheva, D. Pinto, D. H. Geschwind,
811 Transcriptome-wide isoform-level dysregulation in ASD, schizophrenia, and bipolar disorder. *Science*. 362,
812 eaat8127 (2018).

813 29. G. A. Brar, J. S. Weissman, Ribosome profiling reveals the what, when, where and how of protein synthesis.
814 *Nat. Rev. Mol. Cell Biol*. 16, 651–664 (2015).

815 30. J. D. Storey, R. Tibshirani, Statistical significance for genomewide studies. *Proc. Natl. Acad. Sci. U.S.A.* 100,
816 9440–9445 (2003).

817 31. G. E. Hoffman, J. Bendl, G. Voloudakis, K. S. Montgomery, L. Sloofman, Y.-C. Wang, H. R. Shah, M. E.
818 Hauberg, J. S. Johnson, K. Girdhar, L. Song, J. F. Fullard, R. Kramer, C.-G. Hahn, R. Gur, S. Marenco, B. K.
819 Lipska, D. A. Lewis, V. Haroutunian, S. Hemby, P. Sullivan, S. Akbarian, A. Chess, J. D. Buxbaum, G. E.
820 Crawford, E. Domenici, B. Devlin, S. K. Sieberts, M. A. Peters, P. Roussos, CommonMind Consortium
821 provides transcriptomic and epigenomic data for Schizophrenia and Bipolar Disorder. *Sci. Data*. 6, 180
822 (2019).

823 32. D. W. Yao, L. J. O'Connor, A. L. Price, A. Gusev, Quantifying genetic effects on disease mediated by assayed
824 gene expression levels. *Nat. Genet*. 52, 626–633 (2020).

825 33. A. N. Barbeira, S. P. Dickinson, R. Bonazzola, J. Zheng, H. E. Wheeler, J. M. Torres, E. S. Torstenson, K. P.
826 Shah, T. Garcia, T. L. Edwards, E. A. Stahl, L. M. Huckins, D. L. Nicolae, N. J. Cox, H. K. Im, Exploring the
827 phenotypic consequences of tissue specific gene expression variation inferred from GWAS summary statistics.
828 *Nat. Commun*. 9, 1825 (2018).

829 34. S. Ripke, B. M. Neale, A. Corvin, J. T. R. Walters, K.-H. Farh, P. A. Holmans, P. Lee, B. Bulik-Sullivan, D. A.
830 Collier, H. Huang, T. H. Pers, I. Agartz, E. Agerbo, M. Albus, M. Alexander, F. Amin, S. A. Bacanu, M.
831 Begemann, R. A. Belliveau Jr, J. Bene, S. E. Bergen, E. Bevilacqua, T. B. Bigdeli, D. W. Black, R.

Bruggeman, N. G. Buccola, R. L. Buckner, W. Byerley, W. Cahn, G. Cai, D. Campion, R. M. Cantor, V. J. Carr, N. Carrera, S. V. Catts, K. D. Chambert, R. C. K. Chan, R. Y. L. Chen, E. Y. H. Chen, W. Cheng, E. F. C. Cheung, S. Ann Chong, C. Robert Cloninger, D. Cohen, N. Cohen, P. Cormican, N. Craddock, J. J. Crowley, D. Curtis, M. Davidson, K. L. Davis, F. Degenhardt, J. Del Favero, D. Demontis, D. Dikeos, T. Dinan, S. Djurovic, G. Donohoe, E. Drapeau, J. Duan, F. Dudbridge, N. Durmishi, P. Eichhammer, J. Eriksson, V. Escott-Price, L. Essioux, A. H. Fanous, M. S. Farrell, J. Frank, L. Franke, R. Freedman, N. B. Freimer, M. Friedl, J. I. Friedman, M. Fromer, G. Genovese, L. Georgieva, I. Giegling, P. Giusti-Rodríguez, S. Godard, J. I. Goldstein, V. Golimbet, S. Gopal, J. Gratten, L. de Haan, C. Hammer, M. L. Hamshere, M. Hansen, T. Hansen, V. Haroutunian, A. M. Hartmann, F. A. Henskens, S. Herms, J. N. Hirschhorn, P. Hoffmann, A. Hofman, M. V. Hollegaard, D. M. Hougaard, M. Ikeda, I. Joa, A. Julià, R. S. Kahn, L. Kalaydjieva, S. Karachanak-Yankova, J. Karjalainen, D. Kavanagh, M. C. Keller, J. L. Kennedy, A. Khrunin, Y. Kim, J. Klovins, J. A. Knowles, B. Konte, V. Kucinskas, Z. Ausrele Kucinskiene, H. Kuzelova-Ptackova, A. K. Kähler, C. Laurent, J. Lee Chee Keong, S. Hong Lee, S. E. Legge, B. Lerer, M. Li, T. Li, K.-Y. Liang, J. Lieberman, S. Limborska, C. M. Loughland, J. Lubinski, J. Lönnqvist, M. Macek Jr, P. K. E. Magnusson, B. S. Maher, W. Maier, J. Mallet, S. Marsal, M. Mattheisen, M. Mattingsdal, R. W. McCarley, C. McDonald, A. M. McIntosh, S. Meier, C. J. Meijer, B. Melegh, I. Melle, R. I. Mesholam-Gately, A. Metspalu, P. T. Michie, L. Milani, V. Milanova, Y. Mokrab, D. W. Morris, O. Mors, K. C. Murphy, R. M. Murray, I. Myin-Germeys, B. Müller-Myhsok, M. Nelis, I. Nenadic, D. A. Nertney, G. Nestadt, K. K. Nicodemus, L. Nikitina-Zake, L. Nisenbaum, A. Nordin, E. O'Callaghan, C. O'Dushlaine, F. A. O'Neill, S.-Y. Oh, A. Olincy, L. Olsen, J. Van Os, C. Pantelis, G. N. Papadimitriou, S. Papiol, E. Parkhomenko, M. T. Pato, T. Paunio, M. Pejovic-Milovancevic, D. O. Perkins, O. Pietiläinen, J. Pimm, A. J. Pocklington, J. Powell, A. Price, A. E. Pulver, S. M. Purcell, D. Quested, H. B. Rasmussen, A. Reichenberg, M. A. Reimers, A. L. Richards, J. L. Roffman, P. Roussos, D. M. Ruderfer, V. Salomaa, A. R. Sanders, U. Schall, C. R. Schubert, T. G. Schulze, S. G. Schwab, E. M. Scolnick, R. J. Scott, L. J. Seidman, J. Shi, E. Sigurdsson, T. Silagadze, J. M. Silverman, K. Sim, P. Slominsky, J. W. Smoller, H.-C. So, ChrisC. A. Spencer, E. A. Stahl, H. Stefansson, S. Steinberg, E. Stogmann, R. E. Straub, E. Strengman, J. Strohmaier, T. Scott Stroup, M. Subramaniam, J. Suvisaari, D. M. Svrakic, J. P. Szatkiewicz, E. Söderman, S. Thirumalai, D. Toncheva, S. Tosato, J. Veijola, J. Waddington, D. Walsh, D. Wang, Q. Wang, B. T. Webb, M. Weiser, D. B. Wildenauer, N. M. Williams, S. Williams, S. H. Witt, A. R. Wolen, E. H. M. Wong, B. K. Wormley, H. Simon Xi, C. C. Zai, X. Zheng, F. Zimprich, N. R. Wray, K. Stefansson, P. M. Visscher, W. Trust Case-Control Consortium, R. Adolfsson, O. A. Andreassen, D. H. R. Blackwood, E. Bramon, J. D.

862 Buxbaum, A. D. Børglum, S. Cichon, A. Darvasi, E. Domenici, H. Ehrenreich, T. Esko, P. V. Gejman, M. Gill,
863 H. Gurling, C. M. Hultman, N. Iwata, A. V. Jablensky, E. G. Jönsson, K. S. Kendler, G. Kirov, J. Knight, T.
864 Lencz, D. F. Levinson, Q. S. Li, J. Liu, A. K. Malhotra, S. A. McCarroll, A. McQuillin, J. L. Moran, P. B.
865 Mortensen, B. J. Mowry, M. M. Nöthen, R. A. Ophoff, M. J. Owen, A. Palotie, C. N. Pato, T. L. Petryshen, D.
866 Posthuma, M. Rietschel, B. P. Riley, D. Rujescu, P. C. Sham, P. Sklar, D. St Clair, D. R. Weinberger, J. R.
867 Wendland, T. Werge, Schizophrenia Working Group of the Psychiatric Genomics Consortium, Psychosis
868 Endophenotypes International Consortium, Biological insights from 108 schizophrenia-associated genetic loci.
869 *Nature*. 511, 421–427 (2014).

870 35. A. F. Pardiñas, P. Holmans, A. J. Pocklington, V. Escott-Price, S. Ripke, N. Carrera, S. E. Legge, S. Bishop, D.
871 Cameron, M. L. Hamshere, J. Han, L. Hubbard, A. Lynham, K. Mantripragada, E. Rees, J. H. MacCabe, S. A.
872 McCarroll, B. T. Baune, G. Breen, E. M. Byrne, U. Dannlowski, T. C. Eley, C. Hayward, N. G. Martin, A. M.
873 McIntosh, R. Plomin, D. J. Porteous, N. R. Wray, A. Caballero, D. H. Geschwind, L. M. Huckins, D. M.
874 Ruderfer, E. Santiago, P. Sklar, E. A. Stahl, H. Won, E. Agerbo, T. D. Als, O. A. Andreassen, M. Bækvad-
875 Hansen, P. B. Mortensen, C. B. Pedersen, A. D. Børglum, J. Bybjerg-Grauholm, S. Djurovic, N. Durmishi, M.
876 G. Pedersen, V. Golimbet, J. Grove, D. M. Hougaard, M. Mattheisen, E. Molden, O. Mors, M. Nordentoft, M.
877 Pejovic-Milovancevic, E. Sigurdsson, T. Silagadze, C. S. Hansen, K. Stefansson, H. Stefansson, S. Steinberg,
878 S. Tosato, T. Werge, GERAD1 Consortium, CRESTAR Consortium, D. A. Collier, D. Rujescu, G. Kirov, M. J.
879 Owen, M. C. O'Donovan, J. T. R. Walters, Common schizophrenia alleles are enriched in mutation-intolerant
880 genes and in regions under strong background selection. *Nat. Genet*. 50, 381–389 (2018).

881 36. M. Lam, C.-Y. Chen, Z. Li, A. R. Martin, J. Bryois, X. Ma, H. Gaspar, M. Ikeda, B. Benyamin, B. C. Brown,
882 R. Liu, W. Zhou, L. Guan, Y. Kamatani, S.-W. Kim, M. Kubo, A. A. A. A. Kusumawardhani, C.-M. Liu, H.
883 Ma, S. Periyasamy, A. Takahashi, Z. Xu, H. Yu, F. Zhu, Schizophrenia Working Group of the Psychiatric
884 Genomics Consortium, Indonesia Schizophrenia Consortium, Genetic Research on 38etwork38renia 38etwork-
885 China and the Netherlands (GREAT-CN), W. J. Chen, S. Faraone, S. J. Glatt, L. He, S. E. Hyman, H.-G. Hwu,
886 S. A. McCarroll, B. M. Neale, P. Sklar, D. B. Wildenauer, X. Yu, D. Zhang, B. J. Mowry, J. Lee, P. Holmans,
887 S. Xu, P. F. Sullivan, S. Ripke, M. C. O'Donovan, M. J. Daly, S. Qin, P. Sham, N. Iwata, K. S. Hong, S. G.
888 Schwab, W. Yue, M. Tsuang, J. Liu, X. Ma, R. S. Kahn, Y. Shi, H. Huang, Comparative genetic architectures
889 of schizophrenia in East Asian and European populations. *Nat. Genet*. 51, 1670–1678 (2019).

890 37. Johnson RJ, Gomez-Pinilla F, Nagel M, Nakagawa T, Rodriguez-Iturbe B, Sanchez-Lozada LG, Tolan DR,
891 Lanaspa MA. Cerebral Fructose Metabolism as a Potential Mechanism Driving Alzheimer's Disease. *Front*
892 *Aging Neurosci*. 2, 560865 (2020).

893 38. Wu Y, Bi R, Zeng C, Ma C, Sun C, Li J, Xiao X, Li M, Zhang DF, Zheng P, Sheng N, Luo XJ, Yao YG.
894 Identification of the primate-specific gene BTN3A2 as an additional schizophrenia risk gene in the MHC loci.
895 *EBioMedicine*. 44:530-541 (2019).

896 39. Korologou-Linden R, Leyden GM, Relton CL, Richmond RC, Richardson TG. Multi-omics analyses of
897 cognitive traits and psychiatric disorders highlights brain-dependent mechanisms. *Hum Mol Genet.* 32(6):885–
898 96 (2021).

899 40. D. Zhou, Y. Jiang, X. Zhong, N. J. Cox, C. Liu, E. R. Gamazon, A unified framework for joint-tissue
900 transcriptome-wide association and Mendelian randomization analysis. *Nat. Genet*. 52, 1239–1246 (2020).

901 41. S. Burgess, S. G. Thompson, Interpreting findings from Mendelian randomization using the MR-Egger
902 method. *Eur. J. Epidemiol*. 32, 377–389 (2017).

903 42. S. Purcell, B. Neale, K. Todd-Brown, L. Thomas, M. A. R. Ferreira, D. Bender, J. Maller, P. Sklar, P. I. W. de
904 Bakker, M. J. Daly, P. C. Sham, PLINK: A Tool Set for Whole-Genome Association and Population-Based
905 Linkage Analyses. *Am. J. Hum. Genet.* 81, 559–575 (2007).

906 43. A. Gkatzionis, S. Burgess, P. J. Newcombe, Statistical methods for cis-Mendelian randomization with two-
907 sample summary-level data. *Genet. Epidemiol*. 47, 3–25 (2023).

908 44. Zou Y, Carbonetto P, Wang G, Stephens M. Fine-mapping from summary data with the "Sum of Single
909 Effects" model. *PloS Genet*. 18(7): e1010299 (2022).

910 45. C. G. Artieri, H. B. Fraser, Evolution at two levels of gene expression in yeast. *Genome Res.* 24 (2014).

911 46. C. J. McManus, G. E. May, P. Spealman, A. Shteyman, Ribosome profiling reveals post-transcriptional
912 buffering of divergent gene expression in yeast. *Genome Res*. 24, 422–430 (2014).

913 47. F. W. Albert, D. Muzzey, J. S. Weissman, L. Kruglyak, Genetic influences on translation in yeast. *PloS Genet*.
914 10, e1004692 (2014).

915 48. B. Li, C. N. Dewey, RSEM: accurate transcript quantification from RNA-Seq data with or without a reference
916 genome. *BMC Bioinformatics*. 12, 323 (2011).

917 49. M. C. Oldham, P. Langfelder, S. Horvath, Network methods for describing sample relationships in genomic
918 datasets: application to Huntington‘s disease. *BMC Syst. Biol.* 6, 63 (2012).

919 50. B. M. Bolstad, R. A. Irizarry, M. Astrand, T. P. Speed, A comparison of normalization methods for high
920 density oligonucleotide array data based on variance and bias. *Bioinformatics*. 19, 185–193 (2003).

921 51. Y. Jiang, G. Giase, K. Grennan, A. W. Shieh, Y. Xia, L. Han, Q. Wang, Q. Wei, R. Chen, S. Liu, K. P. White,
922 C. Chen, B. Li, C. Liu, DRAMS: A tool to detect and re-align mixed-up samples for integrative studies of
923 multi-omics data. *PloS Comput. Biol.* 16, e1007522 (2020).

924 52. B. Langmead, S. L. Salzberg, Fast gapped-read alignment with Bowtie 2. *Nat. Methods*. 9, 357–359 (2012).

925 53. Y. Liao, G. K. Smyth, W. Shi, featureCounts: an efficient general purpose program for assigning sequence
926 reads to genomic features. *Bioinformatics*. 30, 923–930 (2014).

927 54. O. Stegle, L. Parts, M. Piipari, J. Winn, R. Durbin, Using probabilistic estimation of expression residuals
928 (PEER) to obtain increased power and interpretability of gene expression analyses. *Nat. Protoc*. 7, 500–507
929 (2012).

930 55. O. Delaneau, H. Ongen, A. A. Brown, A. Fort, N. I. Panousis, E. T. Dermitzakis, A complete tool set for
931 molecular QTL discovery and analysis. *Nat. Commun*. 8, 15452 (2017).

932 56. B. L. Pierce, S. Burgess, Efficient Design for Mendelian Randomization Studies: Subsample and 2-Sample
933 Instrumental Variable Estimators. *Am. J. Epidemiol.* 178, 1177–1184 (2013).

934 **Acknowledgments**

We thank Majd Alsayed, Miguel Brown, Dominic Fitzgerald, Amber Thomas, and Mimi Brown for their assistance with RNA-Seq data production and processing. We thank Richard Kopp at SUNY Upstate Medical University for his help with wordsmithing. We thank all of the donors and their relatives participated in the brain collections at Stanley Medical Research Institute and Banner Sun Health Research Institute. We thank Drs. Maree J. Webster and Thomas Beach for their supports to make the tissue available. We thank the High Performance Computing Center of Central South University for partial support of calculation.

Funding:

SUNY Empire Innovation Program

National Institutes of Health grants U01MH122591

National Institutes of Health grants U01MH116489

National Institutes of Health grants R01MH110920

National Institutes of Health grants R01MH126459

National Institutes of Health grants U01MH103340

National Institutes of Health grants R01MH109715

National Institutes of Health grants R01MH110555

National Institutes of Health grants R21MH129817

National Institutes of Health grants R01GM139980

National Natural Science Foundation of China (Grants Nos. 82022024, 31970572)

science and technology innovation Program of Hunan Province (2021RC4018, 2021RC5027)

Author contributions:

Conceptualization: CL, KPW, JP, SHW, BL, XW

Methodology: AWS, LC, DZ, FW, MX, MN, DP, YJW, RV, CZ, KG, GG

Investigation: SHW, QL, YJ, CC, CY, AWS

Visualization: QL

Supervision: SHW, CL, CC, BL, KPW

Writing—original draft: SHW, QL, YJ, CL

Writing—review & editing: SHW, CL, CC, QL

Competing interests: Authors declare that they have no competing interests.

Data and materials availability: All raw data from psychENCODE BrainGVEX project are described in https://www.synapse.org/#!Synapse:syn5613798. All code, materials and results used in the analyses are available in https://www.synapse.org/#!Synapse:syn51664324. All data are available in the main text or the supplementary materials.

Figures and Tables

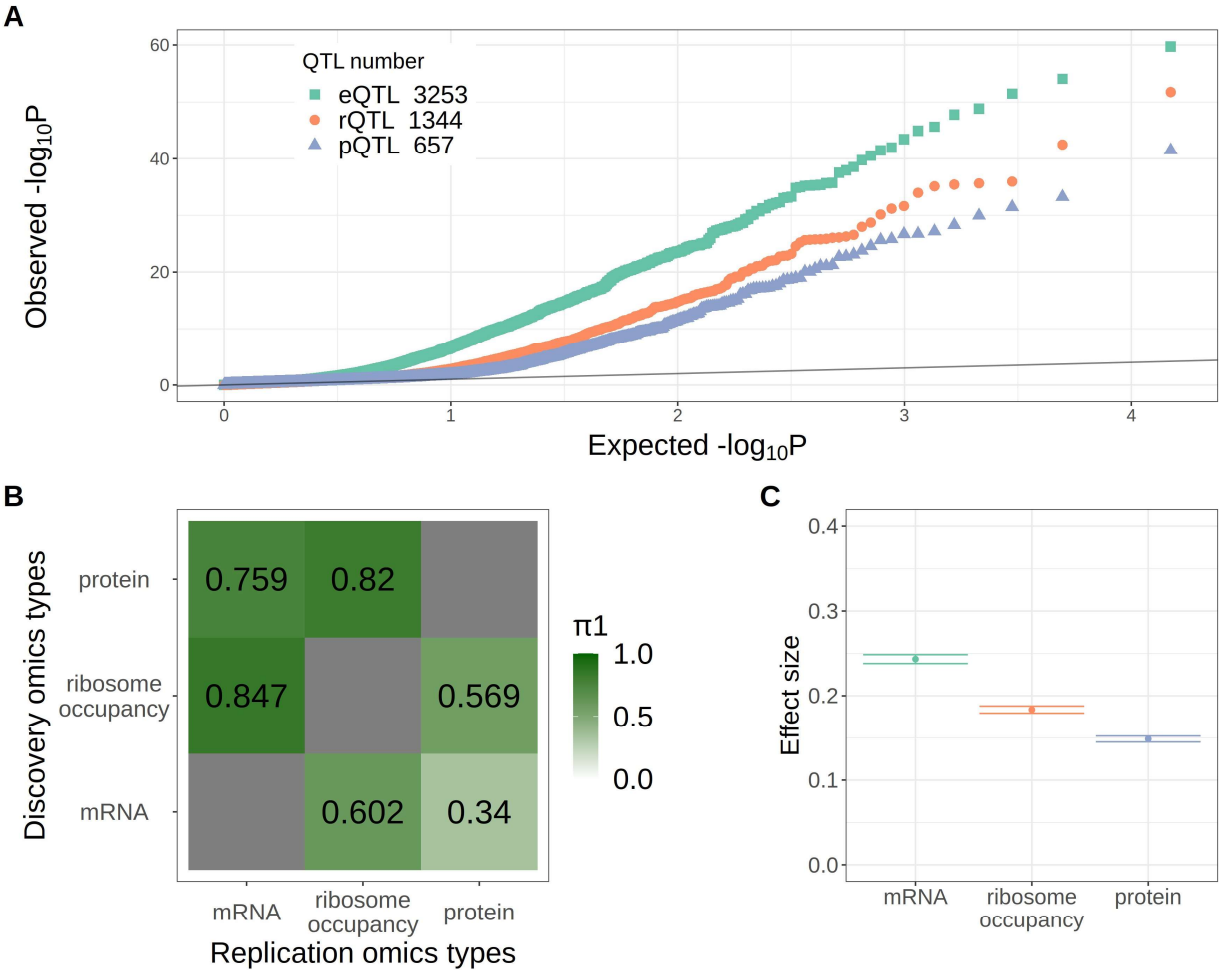

Fig. 1. Genetic regulation of gene expression in the human brain. (A) P-value quantile-quantile plot between the observed (Y-axis) and the expected based on null distribution (X-axis). The black line indicates the expected distribution of p values when there are no real QTL signals. The number of cis-QTLs (i.e. the most significantly associated SNP for each gene) identified at 10% FDR is labeled in the top left inset. **(B)** Replication rate between QTL types. Proportions of QTLs replicated in the other two omics types are listed in the 3X3 matrix. Each row is a discovery omics type and each element of the row correspond to the proportion QTL signals replicated in the omics type specified by the column label. For example, only 34% of the eQTL signals were replicated in the protein data. **(C)** Effect size of CMC eQTL SNPs in BrainGVEX data. Mean and

982 95% confidence interval of absolute per allele effect across all CMC eQTL SNPs that were also

983 analyzed in the BrainGVEX union set is shown.

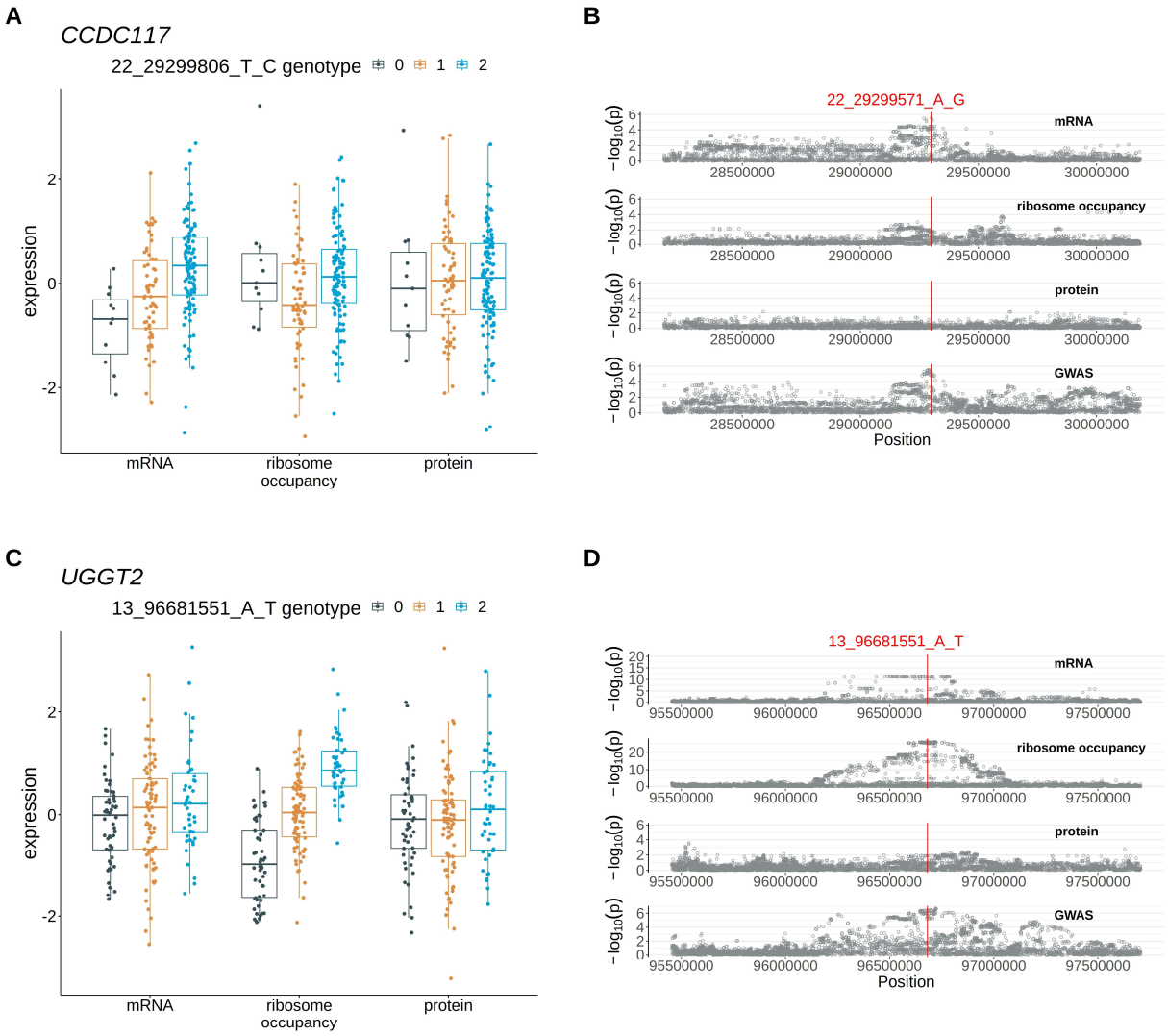

Fig. 2. Signal colocalization between schizophrenia GWAS and omics-specific QTLs. (A, C) Boxplots summarizing normalized gene expression level stratified by QTL genotypes for *CCDC117* esQTLs (A) and *UGGT2* rsQTLs (C). **(B, D)** Manhattan plots showing p value distribution for each QTL type and schizophrenia GWAS for the 1Mb QTL mapping window flanking *CCDC117* (B) and *UGGT2* (D). The red line indicates the position of the lead colocalization SNP between omics-specific QTLs and schizophrenia GWAS.

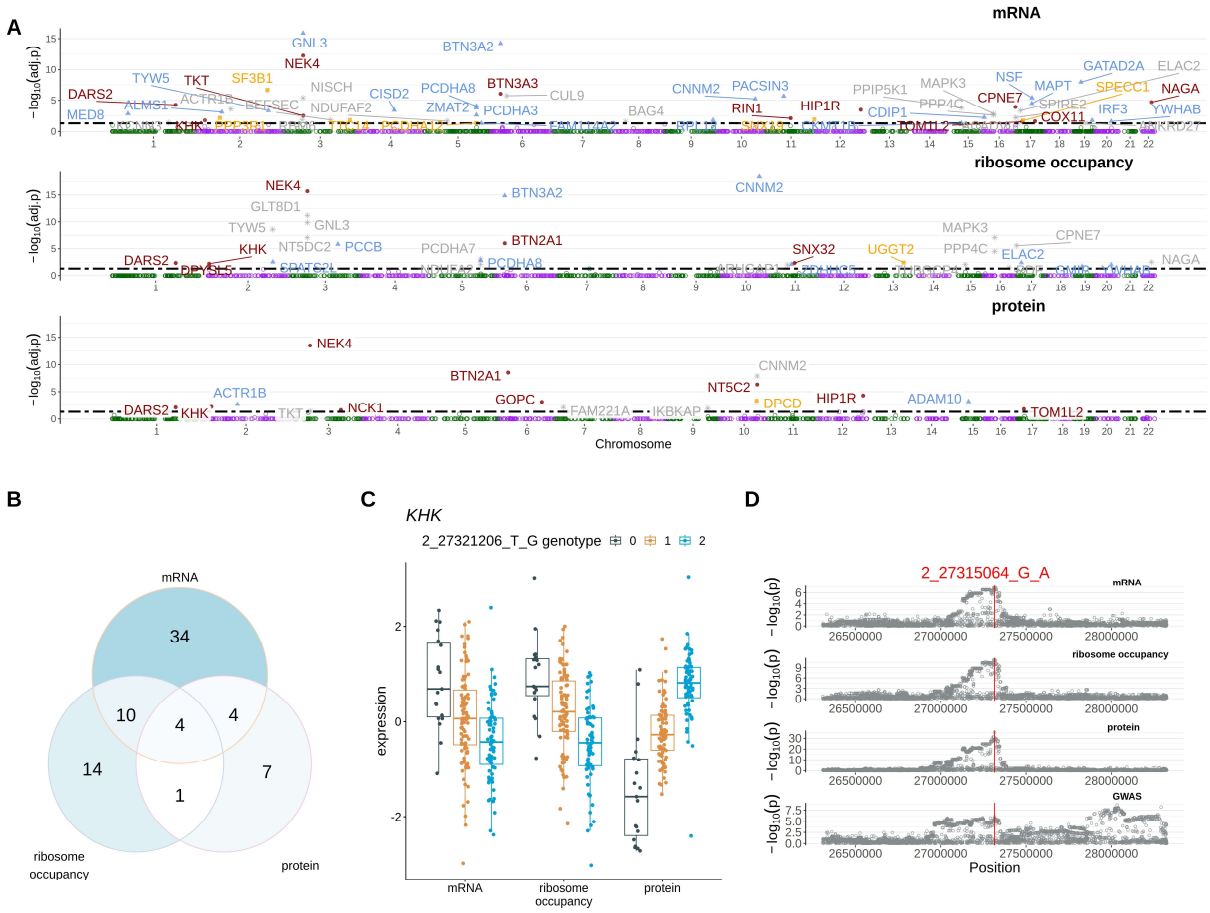

Fig. 3. Schizophrenia risk genes identified from each of the three omics types RNA-Seq (mRNA), ribo-seq (ribosome occupancy), and proteomics (protein) using S-PrediXcan. (A) Manhattan plots showing significance level (i.e. -log10 FWER from S-PrediXcan) of gene-schizophrenia association across the genome for genes that pass the 5% FWER significance cutoff. The black horizontal dotted line indicated the significance cutoff. Risk genes are color-coded according to the MR test results. Grey asterisks mark the risk genes that failed the two-sample MR tests; dark red solid circle marks the risk genes that pass both one-sample MR tests (passing both one-sample MR tests suggest that transcriptionally regulated protein level differences between individuals drives the disease risk); blue triangle marks the risk genes that pass one of the two one-sample MR tests; orange rectangle marks the risk genes that failed both

1005 one-sample MR tests. **(B)** Venn diagram illustrating the number and corresponding percentage of
1006 overlapping risk genes between omics types. **(C)** Boxplots summarizing normalized gene
1007 expression level stratified by eQTL genotypes for *KHK*. **(D)** Manhattan plots showing p value
1008 distribution for each QTL type and schizophrenia GWAS for the 1Mb QTL mapping window
1009 flanking *KHK*. The red line indicates the position of the lead colocalization SNP between eQTLs
1010 and schizophrenia GWAS.
1011

1012

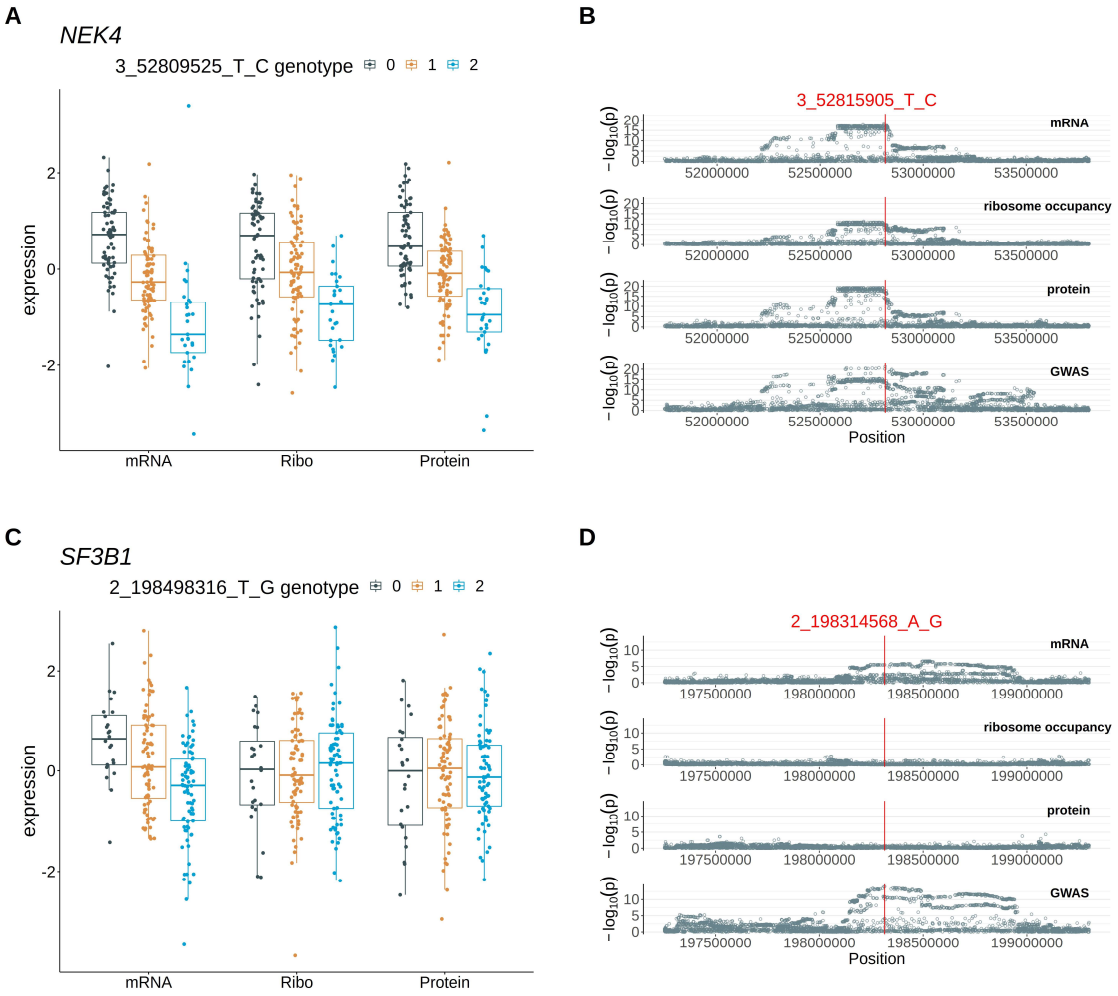

1013

1014 **Fig. 4. Signal colocalization between schizophrenia GWAS and eQTLs of example risk**

1015 **genes**. **(A, C)** Boxplots summarizing normalized gene expression level stratified by QTL

1016 genotypes for *NEK4* eQTLs (A) and *SF3B1* eQTLs (C). **(B, D)** Manhattan plots showing p value

1017 distribution for each QTL type and schizophrenia GWAS for the 1Mb QTL mapping window

1018 flanking *NEK4* (B) and *SF3B1* (D). The red line indicates the position of the colocalization lead

1019 SNP between eQTLs and schizophrenia GWAS.

1020